AMERICAN SOCIETY FOR MICROBIOLOGY | Applied and Environmental Microbiology®

METHODS

Relative Performance of MinION (Oxford Nanopore Technologies) versus Sequel (Pacific Biosciences) Third-Generation Sequencing Instruments in Identification of Agricultural and Forest Fungal Pathogens

Kaire Loit,[a] Kalev Adamson,[b] Mohammad Bahram,[c] Rasmus Puusepp,[d] Sten Anslan,[e] Riinu Kiiker,[a] Rein Drenkhan,[b] Leho Tedersoo[d,f]

[a]Institute of Agricultural and Environmental Sciences, Estonian University of Life Sciences, Tartu, Estonia
[b]Institute of Forestry and Rural Engineering, Estonian University of Life Sciences, Tartu, Estonia
[c]Department of Ecology, Swedish University of Agricultural Sciences, Uppsala, Sweden
[d]Institute of Ecology and Earth Sciences, University of Tartu, Tartu, Estonia
[e]Zoological Institute, Technische Universität Braunschweig, Braunschweig, Germany
[f]Natural History Museum, University of Tartu, Tartu, Estonia

ABSTRACT Culture-based molecular identification methods have revolutionized detection of pathogens, yet these methods are slow and may yield inconclusive results from environmental materials. The second-generation sequencing tools have much-improved precision and sensitivity of detection, but these analyses are costly and may take several days to months. Of the third-generation sequencing techniques, the portable MinION device (Oxford Nanopore Technologies) has received much attention because of its small size and possibility of rapid analysis at reasonable cost. Here, we compare the relative performances of two third-generation sequencing instruments, MinION and Sequel (Pacific Biosciences), in identification and diagnostics of fungal and oomycete pathogens from conifer (Pinaceae) needles and potato (*Solanum tuberosum*) leaves and tubers. We demonstrate that the Sequel instrument is efficient for metabarcoding of complex samples, whereas MinION is not suited for this purpose due to a high error rate and multiple biases. However, we find that MinION can be utilized for rapid and accurate identification of dominant pathogenic organisms and other associated organisms from plant tissues following both amplicon-based and PCR-free metagenomics approaches. Using the metagenomics approach with shortened DNA extraction and incubation times, we performed the entire MinION workflow, from sample preparation through DNA extraction, sequencing, bioinformatics, and interpretation, in 2.5 h. We advocate the use of MinION for rapid diagnostics of pathogens and potentially other organisms, but care needs to be taken to control or account for multiple potential technical biases.

IMPORTANCE Microbial pathogens cause enormous losses to agriculture and forestry, but current combined culturing- and molecular identification-based detection methods are too slow for rapid identification and application of countermeasures. Here, we develop new and rapid protocols for Oxford Nanopore MinION-based third-generation diagnostics of plant pathogens that greatly improve the speed of diagnostics. However, due to high error rate and technical biases in MinION, the Pacific BioSciences Sequel platform is more useful for in-depth amplicon-based biodiversity monitoring (metabarcoding) from complex environmental samples.

KEYWORDS PacBio Sequel, molecular diagnostics, metabarcoding, metagenomics, fungal plant pathogens, needle pathogens, oomycetes, potato, *Solanum tuberosum*, Oxford Nanopore MinION, plant pathogens

Citation Loit K, Adamson K, Bahram M, Puusepp R, Anslan S, Kiiker R, Drenkhan R, Tedersoo L. 2019. Relative performance of MinION (Oxford Nanopore Technologies) versus Sequel (Pacific Biosciences) third-generation sequencing instruments in identification of agricultural and forest fungal pathogens. Appl Environ Microbiol 85:e01368-19. https://doi.org/10.1128/AEM.01368-19.

Editor Irina S. Druzhinina, Nanjing Agricultural University

Address correspondence to Leho Tedersoo, leho.tedersoo@ut.ee.

K.L., K.A., M.B., and R.P. contributed equally to this work.

Received 20 June 2019
Accepted 18 August 2019
Accepted manuscript posted online 23 August 2019
Published 16 October 2019

Fungal and oomycete pathogens and hexapod pests cause enormous losses in agriculture and forestry. Rapid and precise identification of these antagonists enables efficient countermeasures and reduces the costs of biocides and losses to disease (1). Direct morphology-based and culture-based diagnoses are often too slow to prevent the spread of disease. Molecular methods such as PCR-based detection with specific oligonucleotide primers, DNA hybridization-based techniques, and DNA sequence analysis are more accurate and can be rapidly applied to infected tissues and environmental materials (2). However, methods using specific oligonucleotide primers or probes lack the capacity to detect species or strains other than those intended or, worse, yield false-positive signals (3). Although the DNA sequences from selected marker genes may provide high taxonomic resolution, Sanger sequencing of PCR products takes 1 to 3 days depending on access to a sequencing laboratory, and it may fail when DNA of several species or polymorphic alleles are amplified (4).

These disadvantages can be overcome by using a metabarcoding approach. Second- and third-generation high-throughput sequencing (HTS) platforms read hundreds of thousands to billions of DNA molecules simultaneously, recovering the targeted taxa when present at low proportions (5, 6). However, library preparation and running of HTS instruments typically take several days, and there may be queues of weeks to months at commercial service providers. Furthermore, a single sequencing run is costly, which renders it unfeasible for rapid identification of pathogens (7). In spite of millions of output reads, the second-generation SOLiD, Roche 454, Illumina, and Ion Torrent platforms suffer from short read length, which is suboptimal for accurate identification of microorganisms because of low taxonomic resolution of 100- to 500-bp marker gene fragments (8, 9). Third-generation sequencing platforms of Pacific Biosciences (PacBio; RSII and Sequel instruments) and Oxford Nanopore Technologies (ONT; MinION, GridION, and PromethION instruments) enable average sequence lengths of >20,000 bases, but this comes at a 5 to 20% error rate (7, 10–12). In PacBio instruments, the built-in circular consensus sequencing generates multiple copies of the same fragment with a highly accurate consensus (13, 14). Therefore, long consensus molecules have been readily used in *de novo* assembly of complex genomes (15) and DNA barcoding (16). PacBio-based metabarcoding analyses provide greater resolution than short-read second-generation HTS tools in bacteria (9, 17, 18) and fungi (12), including plant pathogens (19).

Compared with other HTS platforms that are represented by large and quite expensive machines, the MinION device is the size of a cell phone and has the cost of a computer, making it affordable to governmental institutions, research laboratories, and small companies (20, 21). Its small size and low power consumption enable carrying the device, a basic analysis toolkit, batteries, and a computer virtually anywhere, as demonstrated by *in situ* sequencing runs in a tropical rain forest (22), Antarctic desert (23), and space station (24). MinION has the capacity to produce >1,000,000 sequences per day, with average read lengths of around 20,000 bases and maximum read lengths approaching 1,000,000 bases (11). Because of low sequence quality, MinION has been used mostly in whole-genome sequencing analyses to resolve long repeats and bridge contigs or to resequence genomes (11, 25). The error rate of reads can be reduced from 10 to 15% to 1 to 5% by sequencing of the complementary strand ($1D^2$ method) or preparing tandem repeat molecules (concatemers), but these solutions are laborious and enable low sequencing depth and, hence, are seldom used (26–29). MinION has been used to generate long DNA barcodes from consensus sequences (30) and to detect specific human pathogens that are easily distinguishable and well represented in reference sequence databases (31, 32). Although multiple reports claim achieving species-level taxonomic resolution in complex environmental samples (33–35), the high error rate renders nanopore sequencing poorly suited for exploratory metabarcoding analyses of natural communities. Conversely, the metagenomics approach has gained popularity for identification of human pathogens to skip the entire PCR step and avoid associated biases (22, 36, 37). Recently, Bronzato Badial et al. (38) demonstrated that plant-pathogenic bacteria and viruses can be

TABLE 1 Detailed information about MinION and Sequel sequencing runs

Run ID	Sample (*n*)	Primer	MinION chemistry	Sequencing cell	DNA quantity (ng)	Sequencing time (min)	No. of reads obtained (% qualified)
ONT1	Pinaceae needles (36)	ITS1catta + ITS4ngsUni	SQK-LSK109	Flow cell 1 (new)	1,165	1,440	1,053,693 (17.7)
Sequel1	Pinaceae needles (36)	ITS1catta + ITS4ngsUni	NA[a]	SMRT cell 1	1,000	600	167,864 (72.6)
ONT2	*Solanum tuberosum* leaves and tubers (35)	ITS1catta + ITS4ngsUni; ITS1Oo + ITS4ngsUni	SQK-LSK109	Flow cell 1 (2nd use)	2,002	343	1,194,242 (3.1)
Sequel2	*S. tuberosum* leaves and tubers (35)	ITS1catta + ITS4ngsUni; ITS1Oo + ITS4ngsUni	NA	SMRT cell 1	1,000	600	177,635 (42.5)
ONT2a	*S. tuberosum* leaves (8)	ITS1catta + ITS4ngsUni	SQK-LSK109	Flow cell 1 (3rd use)	1,076	260	130,130 (10.9)
ONT2b	*S. tuberosum* leaves (8)	ITS1catta + ITS4ngsUni	SQK-LSK109	Flow cell 2 (new)	926	NA	Failed
ONT2f	*S. tuberosum* leaves (8)	ITS1catta + LR14	SQK-LSK308	Flow cell 3 (new)	473	75	5433 (4.9)
ONT2g	*S. tuberosum* tuber (1)	Metagenome	SQK-RAD004	Flow cell 2 (2nd use)	69	251	466,488 (14.2)
ONT2h	*S. tuberosum* tuber (1)	ITS1catta + LR11	SQK-LSK109	Flow cell 2 (3rd use)	448	165	767,611 (44.7)
ONT2i	*S. tuberosum* tuber (1)	Metagenome	SQK-RAD004	Flow cell 4 (new)	31	50	1142 (38.2)
ONT2j	*S. tuberosum* leaf (1)	Metagenome	SQK-RAD004	Flow cell 5 (new)	428	105	107,613 (48.8)
ONT2k	*Cucumis sativa* roots (1)	Metagenome	SQK-RAD004	Flow cell 5 (2nd use)	53	125	5044 (80.2)
ONT2l	*C. sativa* leaf (1)	Metagenome	SQK-RAD004	Flow cell 5 (3rd use)	80	95	23,093 (57.1)
ONT2m	*C. sativa* leaf (1)	Metagenome	SQK-RAD004	Flow cell 5 (4th use)	48	90	1074 (20.8)
ONT2n	*S. tuberosum* stem (1)	Metagenome	SQK-RAD004	Flow cell 6 (new)	56	74	51,175 (47.7)

[a]NA, not applicable.

detected using MinION, whereas Hu et al. (39) extended this to fungal pathogens of cereals.

The main objective of this study was to develop protocols for metabarcoding-based and metagenomics-based detection of fungal and oomycete plant pathogens using third-generation sequencing tools. In particular, we aimed to (i) test the relative biases and shortfalls of MinION-based and PacBio Sequel-based identification and evaluate the perspectives of these methods and (ii) test MinION protocols for ultrarapid pathogen identification. We performed several HTS runs using MinION and Sequel instruments and compared these results to Sanger sequencing, species-specific oligonucleotide-based PCR, and morphology-based identification where relevant. We tested the third-generation HTS methods in two plant pathosystems, conifer (Pinaceae) needles and potato (*Solanum tuberosum* L.) leaves and tubers.

RESULTS

Technical features of MinION and Sequel runs. We compared two MinION runs (ONT1 and ONT2) and two corresponding Sequel runs (Sequel1 and Sequel2) from the same pools of amplicon samples (needles of Pinaceae spp. and various tissues of *S. tuberosum* for both methods) in their technical performance and ability to recover the diversity of Fungi and Oomycota. Compared with Sequel, MinION had severalfold-greater initial sequencing depth, which further depended on the loaded DNA content and sequencing time (considering all MinION runs) (Table 1). The high sequencing depth of MinION was reduced severalfold during the quality filtering and demultiplexing, reaching a level comparable to that of Sequel. Among individual samples within libraries, variation in sequencing depth was slightly greater in MinION (coefficient of variation [CV], 67.8% to 93.4%) than in Sequel (62.8% to 64.5%). The Pearson correlation coefficient of sequencing depth (quality-filtered reads) of samples in MinION and Sequel ranged from 0.585 in the *S. tuberosum* data set ($n = 35$) to 0.853 in the Pinaceae species data set ($n = 36$), suggesting a substantial library preparation or sequencing bias in the former amplicon pool.

For the MinION data sets, chimeras (i.e., artificial reads originating from >1 parent or concatemers of the same read) were detected using the reference-based method of UCHIME but not the *de novo* method of the same program. Putatively chimeric molecules contributed 1.5 to 1.8% to the mapped reads, but nearly half of these were false positives based on manual checking. Interestingly, nearly half of the true chimeras (0.4% of all reads) included parents from different samples, indicating some chimera formation during the library preparation or sequencing process in addition to PCR.

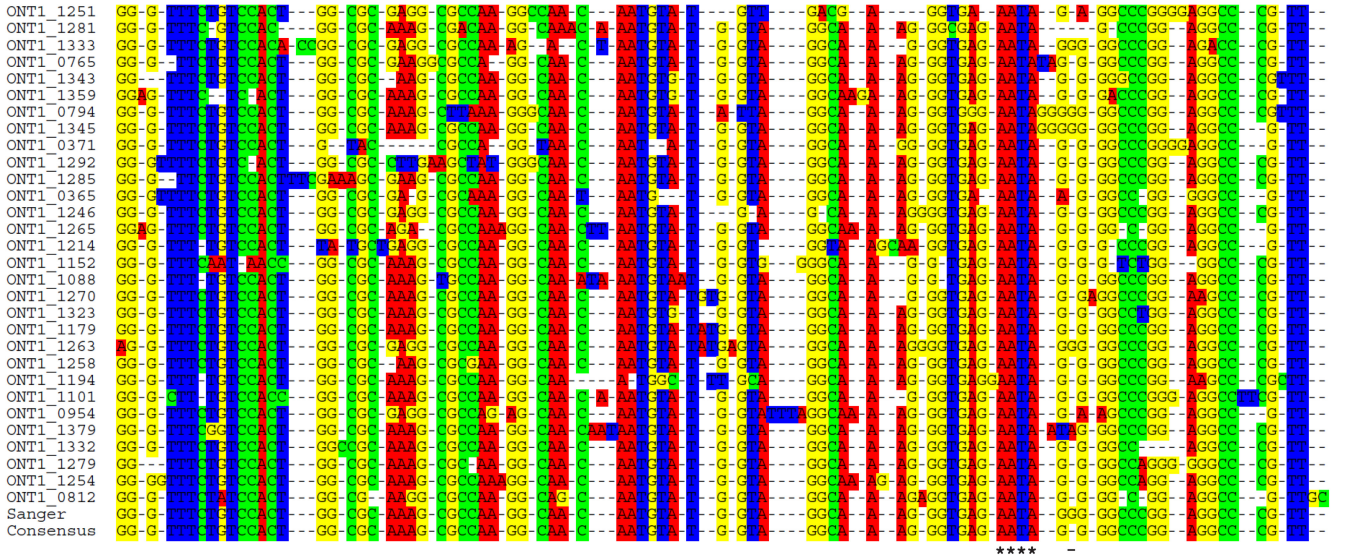

FIG 1 Screenshot example of multiple-sequence alignment of MinION reads mapped to the corresponding Sanger sequence of *Lophodermium pinastri*. Difference from the consensus is indicated with a dash; the accurately sequenced tetramer is indicated with asterisks.

Further manual inspection of demultiplexed sequences revealed that 5 to 8% of all chimeras are self-chimeric, i.e., 1.5-fold to 6-fold concatemeric repeats of itself. In the Sequel data sets, chimeras accounted for 1.9 to 3.7% of reads (including 1.5 to 2.4% detected *de novo*), with no self-chimeric reads remaining in the quality-filtered data.

The index switching (i.e., post-PCR chimeras, where sample molecular identifiers are attached to another molecule in the DNA library) rate was much greater in MinION (3.6% of reads in ONT2 run) than in Sequel (0.14% in Sequel2 run). Based on positive-control samples, we estimated that the error rate in Sequel runs is 0.1% (corresponds to polymerase errors) but 11 to 16% (depending on species) for the conventional 1D method and 11% for the $1D^2$ method (run ONT2f) of MinION. Alignments of hundreds of positive-control and other common sequence types revealed that errors are non-randomly distributed, i.e., occasionally there were no errors across 3 or 4 bases of the alignment, whereas homopolymeric sites exhibited large amounts of combined indels and substitutions (Fig. 1). Because of these nonrandom errors, we were able to construct consensus at 98.5 to 99.5% accuracy (only deletions remaining) with 100 or more reads using MinION. Conversely, most of the individual sequences of Sequel were identical to the Sanger sequences.

All MinION runs using one batch of R9.4 flow cells (1 and 2, accommodating runs ONT1, ONT2, ONT2a, ONT2g, and ONT2h; Table 1) were contaminated by a *Coniothyrium* sp. (INSD accession number JX320132), but this ascomycete was not observed in negative-control samples, other batches or flow cell types, or Sequel. At least partly because of this, the dominant fungal taxa recovered in samples differed in the MinION and Sequel runs (Tables 2 and 3).

Metabarcoding analyses of MinION and Sequel. The MinION run ONT1 included diseased and asymptomatic needle samples of Pinaceae spp. and pure cultures of fungal pathogens. Of the 792,748 "passed" reads, 189,150 (23.9%) were demultiplexed and 183,343 (23.1%) were mapped to reference sequence databases based on the quality criteria (E value of $<e^{-40}$ and sequence similarity of >75%). The ITS1catta-ITS4ngsUni primer pair amplified mostly fungal DNA (99.9% of identified reads). Best hits were distributed across 2,483 fungal molecular operational taxonomic units (MOTUs), with the well-known conifer pathogens yielding hits to 1 or 2 different accession numbers. On average, samples hosted 203.4 ± 130.5 (mean ± standard deviation [SD]) MOTUs. Best hits to the contaminant *Coniothyrium* sp. (Ascomycota) contributed 26.3% of all sequences on average. Of the expected Pinaceae-associated taxa, *Hormonema*

TABLE 2 Identification of fungi in Pinaceae species needle samples

Sample ID	Species-specific primer(s)	Reads (%) per sample[a] (dominant taxa)	
		Sequel	MinION
115	Negative	LoPi, 35; CoTu, 27; RhySp, 3	CoSp 44; CoTu, 21; HeJu, 2
117	Negative	LoCo, 49; DiSp, 25; ViVi, 9	LoCo, 42 DiSp, 13; CoSp, 12
118	LeAc	NeGe, 36; DiSp, 10; HoMa, 9	NeGe, 32; CoSp, 9; DiSp, 6
119	Negative	LoPi, 34; RhySp, 16; CySp, 11	CoSp, 49; ChaeSp, 9; PhEu, 3
123	Negative	DiSp, 49; PlOs, 19; HoMa, 19	DiSp, 25; PlOs, 14; HoMa, 14
125	Negative	HoMa, 56; ViVi, 8; SpRu, 7	HoMa, 49; CoSp, 13; MyTa, 5
127	DoSe	LaCa, 68; HoMa, 25; InSp, 6	LaCa, 67; HoMa, 21; CoSp, 2
139	Negative	MyTa, 22; AuPu, 12; LaCa, 8	MyTa, 20; CoSp, 18; AuPu, 11
141	Negative	DiSp, 21; HoMa, 21; SpRu, 16	HoMa, 17; DiSp, 12; CoSp, 10
142	Negative	LoPi, 40; NeGe, 28; DoSe, 9	CoSp, 43; NeGe, 12; DoSe, 7
148	Negative	MyTa, 40; HeJu, 35; SpRu, 15	HeJu, 37; MyTa, 35; SpRu, 9
154	Negative	ViVi, 18; LoCo, 13; HeJu, 12	CoSp, 31; HeJu, 12; LoCo, 10
2404	NA	DoPi, 100	DoPi, 76; CoSp, 9; PsOp, 2
3904	NA	LeAc, 52; AlAl, 23; HaOr, 23	LeAc, 44; CoSp, 24; AlIr, 19
3906	NA	DoPi, 100	DoSe, 70; CoSp, 7; DoPi, 4
4154	DoPi, DoSe, LeAc	LoPi, 94; AnCo, 3; NeGe, 1	CoSp, 86; AnCo, 3; HoMa, 1
4162	Negative	LoPi, 62; DoSe, 9; CeFe, 6	CoSp, 57; CeFe, 10; DoSe, 9
4180	DoSe	DoSe, 32; LoPi, 22; MyTa, 18	DoSe, 27; CoSp, 26; MyTa, 21
4181	Negative	LoPi, 63; LoSp, 6; LoCo, 5	CoSp, 62; LoSp, 6; LoCo, 5
4192	DoSe	LoPi, 32; PhLa, 18; CyMi, 13	CoSp, 33; PhLa, 13; CyMi, 10
4194	LeAc	TrSp, 44; NeGe, 15; RhiSp, 11	TrSp, 40; NeGe, 8; ScSp, 7
4195	LeAc	HoMa, 52; LoPi, 11; TrSp, 10	HoMa, 44; CoSp, 15; TrSp, 10
4197	DoSe	LoPi, 46; DoSe, 25; RhySp, 8	CoSp, 49; DoSe, 19; LoPi, 14
4220	Negative	LoPi, 58; AnSp, 32; PhLa, 5	CoSp, 56; AnSp, 28; PhLa, 3
4221	DoSe	LoPi, 47; MyTa, 43; AuPu, 3	CoSp, 47; MyTa, 37; DoSe, 4
4222	DoSe	LoPi, 48; DoSe, 7; EuSp, 6	CoSp, 49; DoSe, 7; PhSp, 5
4223	DoSe, LeAc	HoMa, 25; DiSp, 10; DoSe, 8	HoMa, 20; CoSp, 8; DoSe, 8
5136	Negative	AsSy, 73; DiVi, 27	AsSy, 36; DiSp, 13; CoSp, 11
5137	Negative	HeAn, 56; DoSe, 32; AsSo 3	HeAn, 45; DoSe, 31; CoSp, 3
5146	Negative	GiTr, 17; DiSp, 17; CeSp, 14	CeSp, 14; PhLa, 11; GiTr, 10
5148	Negative	DiSp, 45; ArSp 11; GiTr, 11	DiSp, 29; DiVi 10; GiTr, 7
5151	Negative	CyMi, 22; MyTa, 11; ClSp, 9	CyMi, 18; CoSp, 15; MyTa, 11
5186	Negative	MyTa, 70; ViVi, 8; DiSp, 5	MyTa, 66; CoSp, 15; AuPu, 4
5194	Negative	DiVi, 26; HelSp, 20; MaOb, 11	DiVi, 17; MyTa, 10; DoSp, 10
5195	Negative	RaHy, 57; ZyVe, 19; ExSp, 18	RaHy, 41; CaSp, 12; ZyVe, 11
5297	Negative	ZyVe, 18; RhiSp, 16; RhMu 5	ZyVe, 17; CoSp, 10; ScSp, 10
5307	Negative	ZyVe, 20; ExSp, 12; MyTa, 10	ZyVe, 13; CoSp, 11; MyTa, 10
14374	ND[b]	LeAc, 38; DoSp, 13; TeSp, 10	LeAc, 31; PeIn, 10; CoSp, 7
14378	ND	HoMa, 46; NeSp, 23; ChSp, 6	HoMa, 42; PlSt, 16; CoSp, 8

[a]Percentages in Sequel and MinION columns indicate the percentage of sequences assigned to particular MOTUs. Abbreviations for species corresponding to dominant MOTUs: AlAl, *Alternaria alternata*; AlIr, *Alternaria iridiaustralis*; AnCo, *Anthostomella conorum*; AnSp, *Anthostomella* sp.; ArSp, *Articulospora* sp.; AsSo, *Ascocoryne solitaria*; AsSy, *Aspergillus sydowii*; AuPu, *Aureobasidium pullulans*; CaSp, Capnodiales sp.; CeFe, *Cenangium ferruginosum*; CeSp, Ceratobasidiaceae sp.; ChSp, *Chalara* sp.; ChaeSp, Chaetothyriales sp.; ClSp, *Cladosporium* sp.; CoSp, *Coniothyrium* sp.; CoTu, *Coleosporium tussilaginis*; CyMi, *Cyclaneusma minus*; CySp, *Cyphellophora* sp.; DiSp, Didymellaceae sp.; DiVi, *Didymella viburnicola*; DoPi, *Dothistroma pini*; DoSe, *Dothistroma septosporum*; DoSp, Dothideomycetes sp.; EuSp, Eurotiomycetes sp.; ExSp, *Extremus* sp.; GiTr, *Gibberella tricincta*; HaOr, *Hannaella oryzae*; HeAn, *Heterobasidion annosum*; HeJu, *Herpotrichia juniperi*; HelSp, Helotiales sp.; HoMa, *Hormonema macrosporum*; InSp, *Insecta* sp.; LaCa, *Lachnellula calyciformis*; LeAc, *Lecanosticta acicola*; LoCo, *Lophodermium conigenum*; LoPi, *Lophodermium pinastri*; LoSp, *Lophodermium* sp.; MaOb, *Malassezia obtusa*; MyTa, *Mycosphaerella tassiana*; NeGe, *Neocatenulostroma germanicum*; NeSp, *Nectria* sp.; PeIn, *Perusta inaequalis*; PhEu, *Phaeococcomyces eucalypti*; PhLa, *Phacidium lacerum*; PhSp, *Phaeomoniella* sp.; PlOs, *Pleurophoma ossicola*; PlSt, *Pleonectria strobi*; RaHy, *Ramularia hydrangeae-macrophyllae*; RhiSp, *Rhizosphaera* sp.; RhMu, *Rhodotorula mucilaginosa*.; RhySp, Rhytismataceae sp.; ScSp, *Scleroconidioma sphagnicola*; SpRu, *Sporobolomyces ruberrimus*; ZyVe, *Zymoseptoria verkleyi*; TeSp, Teratosphaeriaceae sp.; TrSp, *Truncatella spadicea*; ViVi, *Vishniacozyma victoriae*.
[b]ND, not determined.

macrosporum (6.2%), *Lophodermium conigenum* (5.0%), and a Didymellaceae sp. (4.3%) (all Ascomycota) yielded the greatest number of hits (Fig. 2A). All of these taxa occurred in 94 to 100% of samples.

The corresponding Sequel run Sequel1 revealed 121,965 demultiplexed reads that were clustered into 535 MOTUs, all above the quality threshold. Samples harbored 51.5 ± 41.6 MOTUs on average, nearly four times less than that in the MinION data set.

TABLE 3 Identification of fungi in *Solanum tuberosum* tissue samples

Sample	Sanger	Reads (%) per sample[a]	
		Sequel	MinION
KL001	Failed	MyTa, 10; BuCr, 8; SpRo, 7	CoSp, 24; CerSp, 16; LeAc, 11
KL002	Failed	KoCh, 27; PeEx, 13; SpRo, 8	DoSe, 27; KoCh, 9; CoSp, 8
KL003	Failed	BuCr, 21; FiSt, 14; ClSp, 12	BuCr, 17; ClSp, 12; CoSp, 11
KL004	Failed	EpNi, 12; MyTa, 10; SpRo, 10	NeGe, 13; CoSp, 11; NeMi, 9
KL005	FiWi	FiWi, 41; DioSp, 5; BuAu, 5	FiWi, 26; MyTa, 13; CoSp, 10
KL006	Failed	SpRo, 17; LeSp, 8; ViVi, 7	CoSp, 15; HoMa, 11; MyTa, 8
KL007	Failed	FiSt, 26; SpSp, 11; MyTa, 7	CoSp, 15; FiSt, 13; SpSp, 7
KL008	Failed	PaLa, 49; SpRo, 9; MyTa, 6	PaLa, 36; CoSp, 14; MyTa, 8
KL009	Failed	DiSp, 15; DiPo, 12; MyTa, 11	DiSp, 12; CoSp, 11; MyTa, 8
KL010	BoEx	BoSp, 47; FiSt, 12; SpRo, 5	BoSp, 26; CoSp, 18; FiSt, 5
KL011	BoEx	BoSp, 71; ExEq, 9; MyTa, 4	BoSp, 52; ExEq, 8; MyTa, 4
KL012	BoEx	BoSp, 96; ViTe, 2; MySp, 1	BoSp, 50; CoSp, 14; HeJu, 3
KL013	DioSp	MyTa, 17; BuCr, 9; ViVi, 8	CoSp, 24; MyTa, 13; HyaSp, 4
KL014	Failed	CyMa, 14; ViVi, 10; LeSp, 7	CoSp, 30; ViVi, 10; CoTu, 6
KL015	BoEx	BoSp, 92; BuCr, 1; FiSt, 1	BoSp, 37; LoCo, 19; CoSp, 8
KL016	Failed	ViVi, 18; PaLa, 15; LeSp, 12	CoSp, 29; PaLa, 10; HoMa, 7
KL017	BoEx	BoSp, 65; FiSt, 8; ViVi, 4	BoSp, 44; CoSp, 15; TrSp, 7
KL018	Failed	MyTa, 35; PlSp, 13; FiSt, 13	CoSp, 39; MyTa, 11; DoSe, 9
KL019	Failed	AuPu, 13; BuCr, 11; ViTe, 11	CoSp, 32; AuPu, 13; BoSp, 7
KL020	BoEx	BoSp, 49; SpSp, 9; FiSt, 9	CoSp, 29; BoSp, 17; SpSp, 5
KL021	Failed	MyTa, 35; ViVi, 15; ClSp, 10	MyTa, 30; CoSp, 20; AuPu, 9
KL022	ClSp	MyTa, 42; BuCr, 13; AuPu, 9	RhMu, 33; MyTa, 23; CoSp, 11
KL023	Failed	AuPu, 42; MyTa, 33; AlAl, 8	CoSp, 46; AnSp, 24; AuPu, 7
KL024	ClSp	MyTa, 51; SpRo, 9; DiBu, 6	MyTa, 29; CoSp, 20; DoSe, 10
KL025	Failed	ViVi, 18; DiSp, 18; ClSp, 13	CoSp, 30; DiSp, 12; ClSp, 8
KL026	ClSp	MyTa, 16; SuGr, 15; BuCr, 12	CoSp, 42; MyTa, 11; AtSp, 5
KL027	DioSp	BuCr, 65; ViVi, 9; MyTa, 7	CoSp, 75; CeFe, 4; BlGr, 3
KL028	Failed	DiSp, 97; HaVe, 3; CuMo, 0	DiSp, 57; PhBu, 6; PlSp, 6
KL029	Failed	DiSp, 54; BoSp, 46; PlCu, 0	DiSp, 32; BoSp, 28; PlSp, 6
KL030	Failed	PlCu, 100	PlCu, 17; ZyVe, 11; ScSp, 8
KL031	Failed	DiSp, 93; PeBi, 4; BoSp, 1	DiSp, 50; PlSp, 6; PhBu, 5
KL032	Failed	PlCu, 43; PsSp, 22; CuMo, 17	PlCu, 23; PlOr, 11; GeAs, 10
KL033	Failed	DeSp, 50; PlCu, 38; NeSp, 11	PlCu, 41; PlSp, 36; NeSp, 8
KL034	Failed	PenSp, 80; PlCu, 11; CuMo, 2	CeSp, 13; PhLa, 12; GiTr, 8
KL035	Failed	PeBi, 41; PenSp, 38; PeBr, 10	PeBi, 42; PeAe, 23; PeBr, 11

[a]Percentages in Sequel and MinION columns indicate the percentages of sequences assigned to particular MOTUs. Abbreviations for species corresponding to dominant MOTUs: AlAl, *Alternaria alternata*; AnSp, *Anthostomella* sp.; AtSp, Atheliaceae sp.; AuPu, *Aureobasidium pullulans*; BlGr, *Blumeria graminis*; BoEx, *Boeremia exigua*; BoSp, *Boeremia* sp.; BuAu, *Buckleyzyma aurantiaca*; BuCr, *Bullera crocea*; CeFe, *Cenangium ferruginosum*; CerSp, *Cercozoa* sp.; CeSp, Ceratobasidiaceae sp.; ClSp, *Cladosporium* sp.; CoSp, *Coniothyrium* sp.; CoTu, *Coleosporium tussilaginis*; CuMo, *Cutaneotrichosporon moniliiforme*; CyMa, *Cystofilobasidium macerans*; DeSp, *Dendryphion* sp.; DiBu, *Dioszegia butyracea*; DioSp, *Dioszegia* sp.; DiPo, *Didymella pomorum*; DiSp, Didymellaceae sp.; CeSp, *Celosporium* sp.; EpNi, *Epicoccum nigrum*; ExEq, *Exophiala equina*; ExPi, *Exobasidium pieridis-ovalifoliae*; FiSt, *Filobasidium stepposum*; FiWi, *Filobasidium wieringae*; GeAs, *Geomyces asperulatus*; GiTr, *Gibberella tricincta*; HaVe, *Harzia velata*; HeJu, *Herpotrichia juniperi*; HoMa, *Hormonema macrosporum*; HyaSp, *Hyaloscyphaceae* sp.; KoCh, *Kondoa changbaiensis*; LaCa, *Lachnellula calyciformis*; LeAc, *Lecanosticta acicola*; LeSp, *Leucosporidium* sp.; LoCo, *Lophodermium conigenum*; MySp, *Mycosphaerellaceae* sp.; MyTa, *Mycosphaerella tassiana*; NeGe, *Neocatenulostroma germanica*; NeMi, *Neocatenulostroma microsporum*; NeSp, *Nectria* sp.; PaLa, *Papiliotrema laurentii*; PeAe, *Penicillium aethiopicum*; PeBi, *Penicillium bialowiezense*; PeBr, *Penicillium brevicompactum*; PeEx, *Penicillium expansum*; PenSp, *Penicillium* sp.; PhBu, *Phoma bulgarica*; PhLa, *Phacidium lacerum*; PlCu, *Plectosphaerella cucumerina*; PlOr, *Plectosphaerella oratosquillae*; PlSp, Pleosporales sp.; PsSp, *Pseudogymnoascus* sp.; RaHy, *Ramularia hydrangeae-macrophyllae*; RhiSp, *Rhizosphaera* sp.; RhMu, *Rhodotorula mucilaginosa*; ScSp, *Scleroconidioma sphagnicola*; SpRo, *Sporobolomyces roseus*; SpSp, *Sporobolomyces* sp.; SuGr, *Suillus granulatus*; ZyVe, *Zymoseptoria verkleyi*; TrSp, *Truncatella spadicea*; ViTe, *Vishniacozyma tephrensis*; ViVi, *Vishniacozyma victoriae*.

Altogether, 99.9% reads were ascribed to fungi, with *L. pinastri* (17.8%), *Dothiostroma septosporum* (8.9%), and *Hormonema macrosporum* (7.0%) (all Ascomycota) dominating across the entire data set (Fig. 2B). These dominant taxa occurred in 43 to 65% of samples.

The ONT MinION run ONT2 recovered 255,137 passed sequences, of which 16.2% were demultiplexed and 14.4% were mapped to reference database reads. Based on the occurrence of Pinaceae-specific pathogens in potato samples, we estimated that

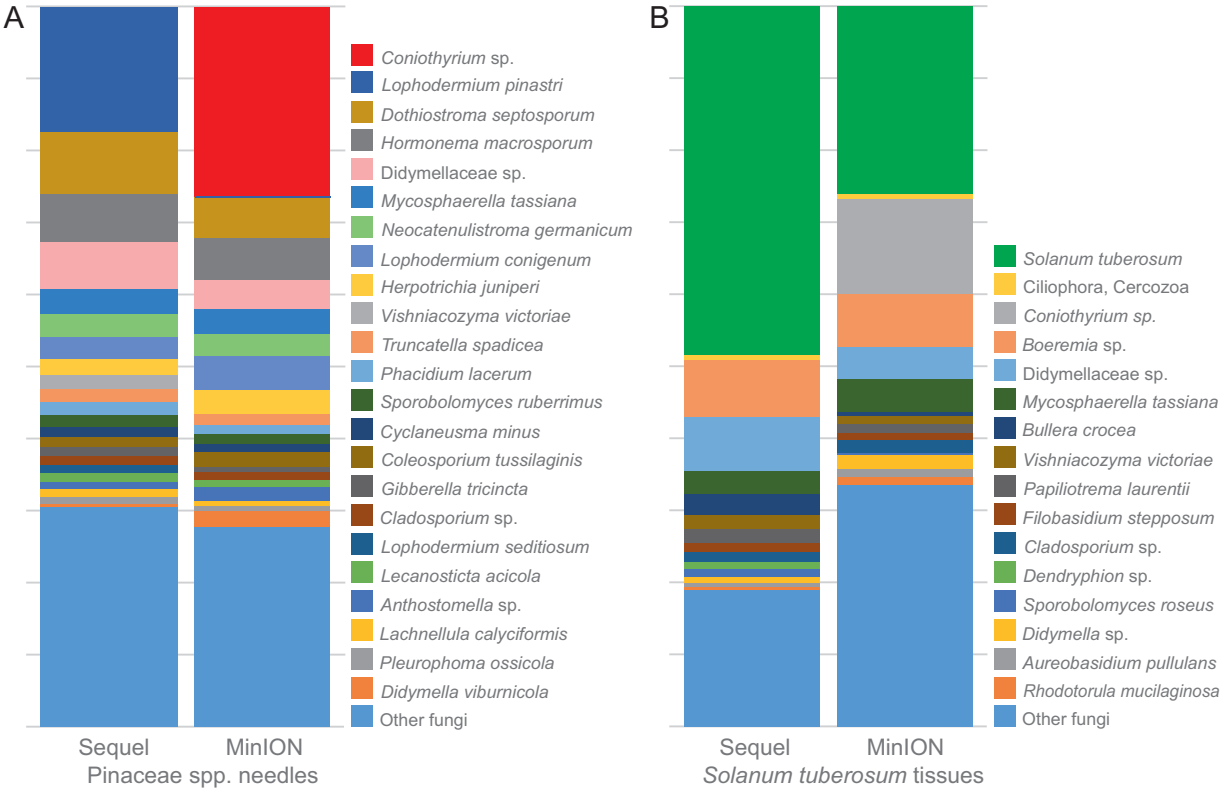

FIG 2 Column diagrams demonstrating relative abundance of MOTUs in Pinaceae species needles (A) and *Solanum tuberosum* leaves and tubers (B) based on the ITS1catta + ITS4ngsUni amplicons as revealed by Sequel and MinION instruments.

13.4% of the reads were carried over from the previous ONT1 run, in which we used the same primer and tag combinations. In the ONT2 run, these Pinaceae-specific MOTUs had proportionally similar relative abundances when compared across the same index combinations. The ITS1catta-ITS4ngsUni forward primer amplified mostly fungi (74.2% of identified reads; Fig. 2B) and plants (26.1% reads corresponding to nine MOTUs of *S. tuberosum*). Of fungi, MOTUs corresponding to *Coniothyrium* sp. (13.2% of reads), *Boeremia* sp. (7.5%), *Mycosphaerella tassiana* (4.6%), and Didymellaceae sp. (4.4%) (all Ascomycota) dominated. The average taxonomic richness was 81.7 ± 43.3 MOTUs per sample. The ITS1Oo-ITS4ngsUni primer pair revealed Oomycota (47.7%), other Heterokonta (19.2%), Fungi (23.6%), and Viridiplantae (9.5%). In each sample, 0 to 3 Oomycota taxa were found, and all of these occurred only once or twice (Table 4). The majority of samples produced no visible amplicon on gel with these primers, and correspondingly, no Oomycota taxa were recovered from these samples based on MinION sequencing.

The Sequel run Sequel2 revealed 75,573 demultiplexed reads that were separated into 308 MOTUs, all matching to reference sequences. On average, 39.6 ± 20.3 MOTUs were recovered per sample. In the ITS1catta-ITS4ngsUni amplicons, Fungi, Viridiplantae, Alveolata, and Rhizaria contributed to 51.0%, 48.4%, 0.5%, and 0.1% of reads, respectively. All plant reads were distributed across 25 MOTUs that were all assigned to *S. tuberosum*. Six of the MOTUs probably represent naturally high variation among the rRNA internal transcribed spacer (ITS) 1 and 2 sequences of *S. tuberosum* (based on INSD entries), whereas others represent pseudogenes or nonfunctional copies. These were rare to common (up to 3% of all variants) and sometimes exceeded the abundance of regular variants in individual samples. Of fungi, the largest number of reads belonged to *Boeremia* sp. (8.0%), Hysteriaceae sp. (7.4%), and *Mycosphaerella tassiana* (3.3%) (all Ascomycota) (Fig. 2B). The ITS1Oo-ITS4ngsUni reads were mostly assigned to Oomycota (62.9%), other Heterokonta (33.9%), Viridiplantae (3.0%), and Alveolata (0.2%). This

TABLE 4 Identification of Oomycota and other Heterokonta in *Solanum tuberosum* tissue samples based on the ITS1Oo + ITS4ngsUni amplicons

	Reads (%) per sample[a]	
Sample	**Sequel**	**MinION**
KL003	*Phytophthora infestans*, 90; *Peronospora radii*, 10	*P. infestans*, 84; *P. radii*, 11
KL004	Xanthophyceae sp., 100	Heterokonta sp., 86
KL005	*Peronospora agrestis*, 73; Xanthophyceae sp., 27	*P. agrestis*, 83; Heterokonta sp., 17
KL006	*Peronospora* sp., 85; *Eustigmatos* sp., 15	*Peronospora* sp., 79; Eustigmataceae sp., 13
KL007	Chromulinaceae sp., 84; *Hyaloperonospora parasitica*, 16	Chromulinaceae sp., 66; *H. parasitica*, 9
KL008	*Peronospora violae*, 100	*P. violae*, 84
KL010	Chromulinaceae sp., 100	Chromulinaceae sp., 93
KL013	*H. parasitica*, 100	*H. parasitica*, 100
KL014	Xanthophyceae sp., 100	Heterokonta sp., 50
KL021	*Peronospora variabilis*, 100	
KL022	*P. variabilis*, 100	
KL024	*P. variabilis*, 100	

[a]Percentages in Sequel and MinION columns indicate the percentages of sequences assigned to particular MOTUs. Samples with no PCR product and no sequences are excluded. Notably, plant and fungal sequences contributed on average 10% to MinION data (probably index switch artifacts from the fungal data set; not shown).

data subset yielded 0 to 2 MOTUs of Oomycota or other Heterokonta per sample (Table 4).

Taking these results together, Sequel and MinION recovered the same dominant fungal species (excluding the contaminant) in 60% and 63% of the Pinaceae spp. (Table 2) and *S. tuberosum* (Table 3) samples, respectively. These values increased to 78% and 83%, respectively, when considering the overlap in the three best-matching taxa. Inspection of the discordant samples revealed that contamination from the previous ONT1 run blurred the results of the *S. tuberosum* samples and MinION produced 1 to 2 orders of magnitude less high-quality reads matching to multiple species, such as *Vishniacozyma victoriae* and a *Cystobasidium* sp. (both Basidiomycota) and *L. pinastri* and a *Dendryphion* sp. (both Ascomycota), than Sequel (Fig. 2). These species had a relatively high proportion of homopolymers (>3-mers) per base compared with dominant but equally shared taxa ($F_{1,8} = 5.79$; $P = 0.088$), which may have reduced their relative abundances after quality filtering of nanopore sequences. The ITS1Oo-ITS4ngsUni data subsets were in stronger agreement in Sequel and MinION, apart from the lack of *Peronospora variabilis* among MinION reads, hence its unsuccessful diagnosis from three *S. tuberosum* leaf samples (Table 4).

The ONT2a MinION run was designed to test whether long indexes reduce index switching. The ONT2a run revealed an index switch rate of 3.8%. *S. tuberosum* (14 MOTUs) contributed to 18.7% of reads, whereas the contaminant *Coniothyrium* sp. accounted for 16.7% of reads, prevailing in half of the eight samples. Of other fungal species, *Papiliotrema laurentii* (11.5%) and *Filobasidium stepposum* (7.0%) (both Basidiomycota) and *Mycosphaerella tassiana* (5.6%) dominated. These species were less common in the same eight samples as recovered in the ONT2 run with regular indexes (3.8%, 2.7%, and 4.6%, respectively). In spite of severalfold differences in relative abundance of MOTUs, the ONT2a and ONT2 runs recovered the same dominant MOTUs in 75% of the samples.

The ONT2f run was intended to test suitability of the $1D^2$ method relative to the conventional 1D method based on ONT2 run. Because the $1D^2$ protocol requires DNA fragments of >3 kb, we sequenced a 3.2-kb amplicon (see Materials and Methods). The ONT2f run recovered only 3,241 $1D^2$ reads, of which 29.7% fell within a 10% interval of the expected read length of ca. 3,200 bases. The median read length was 954 bases. As the positive-control sample revealed no reads, the index switch rate could not be calculated. Of all sequences, *S. tuberosum* (17 MOTUs) accounted for 54.2% of them. Of fungi (39.8%), *Taphrina populina* (6.0%), *Parastagonospora* sp. (3.8%), and *Glarea lozoyensis* (3.0%) (all Ascomycota) dominated. These species were much less common in the ONT2 library (0.1%, <0.1%, and <0.1%, respectively). The same species were among the dominants in only 25% of samples based on the ONT2 and ONT2f runs. It remains

unknown whether these biases are related to sequencing of long amplicons or the 1D^2 method.

Metabarcoding versus metagenomics approach and sequence quality bins. We designed two MinION runs to compare the relative performance of the metagenomics approach (ONT2g) and metabarcoding approach (ONT2h) using a single diseased *S. tuberosum* tuber sample, KL036 (Table 1). The ONT2g metagenomics run yielded 66,133 and 400,355 passed and failed reads, respectively. The 5,000 randomly selected sequences from each of these bins revealed 1,325 passed reads and 1 failed read that met our quality standards (see Materials and Methods). Altogether, 37.4% of the passed reads represented sequences carried over from a previous run. After removal of these reads, the metagenomics data set was dominated by plant and bacterial reads. Best hits to *Lycopersicon esculentum* (tomato, 29.0% of reads) and seven species of *Solanum* (altogether, 22.6%) collectively represented *S. tuberosum*. Of bacteria, hits to *Agrobacterium tumefaciens* (10.5%), *Variovorax paradoxus* (9.7%), and *Sphingopyxis alaskensis* (3.8%) dominated. Fungal hits were less common; those to *Thanatephorus cucumeris* (1.6%; Basidiomycota) and *Boeremia exigua* (1.0%) prevailed. Of these best-matching taxa, the bacterial species *A. tumefaciens* and *V. paradoxus* are probably present given their strongest hits of 93% and 92% and average hits of 87% and 85% sequence similarity, respectively, to reference strains. Conversely, the particular species *S. alaskensis*, *B. exigua*, and *T. cucumeris* are probably absent, because their best hits reached 84%, 88%, and 86%, and all hits averaged 79%, 80%, and 80% similarity to reference sequences, respectively, suggesting that these MOTUs correspond to other species in these genera that have no genomic information available.

The ONT2h run represented a long amplicon of the same sample, recovering 342,923 passed reads and 423,688 failed reads. Of the randomly selected 5,000 sequences for each bin, 1,876 passed reads and 1,068 failed reads met the quality threshold (see Materials and Methods). The positive control used in the next-to-previous run accounted for 0.2% of all sequences, mostly in the failed bin. Out of the 18 most abundant MOTUs, the proportion of 11 MOTUs differed significantly ($P < 0.001$) among the passed and failed bins, indicating that reads of certain taxa are much more likely to be recorded as failed. Of the passed reads, matches to *Lignincola laevis* (64.3%) and *Verticillium biguttatum* (5.0%) (both Ascomycota) and *T. cucumeris* (3.0%) dominated. In the failed bin, *V. biguttatum* (19.9%), *L. laevis* (15.7%), and *Plectosphaerella cucumerina* (7.8%) (all Ascomycota) prevailed, followed by *T. cucumeris* (6.0%). Of the dominant taxa recovered, only *V. biguttatum*, *T. cucumeris*, and *P. cucumerina* were identified to the species level given their high maximum (>90%) and mean (>85%) sequence similarity to the reference. We tested whether the taxa relatively more abundant in the failed bin possess more homopolymers than those in the passed bin, but there was no significant relationship between the relative abundance of taxa in these bins and the proportion of 4-mers per base ($F_{1,9} = 2.23$; adjusted $R^2 = 0.110$; $P = 0.169$).

In the ONT2g metabarcoding and ONT2h metagenomics data sets derived from the same *S. tuberosum* sample, *T. cucumeris* was the only shared taxon. Other fungal species common in the metabarcoding data set were absent from the metagenomics data set, probably because their genomes are unavailable. Several of these ascomycetes may have best matches to *B. exigua*, the genome of which has been sequenced. This situation highlights limitations of the metagenomics approach when insufficient reference data are available.

Rapid pathogen diagnostics. We aimed to minimize the time from sample preparation to diagnosis based on MinION sequencing of metagenomes using multiple samples (see Materials and Methods). In particular, we reduced the lysis and centrifugation time in DNA extraction and purification protocols and limited sequencing time (Fig. 3).

For the ONT2i run, we used bead beating combined with Phire lysis and FavorPrep purification to obtain DNA from a single diseased *S. tuberosum* tuber sample. MinION

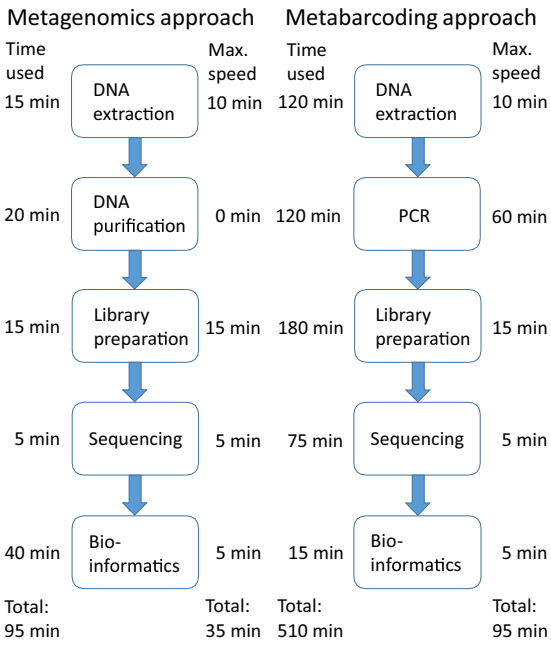

FIG 3 Schematic overview of work flow and speed of pathogen diagnostics in this study (time used) and maximum potential speed under optimal conditions using metagenomics and metabarcoding approaches with the MinION instrument. Note that the time used here was compiled across our successful runs and does not indicate any individual analyses.

sequencing revealed *L. esculentum* (72.2% of sequences), *S. tuberosum* (14.4%), and *T. cucumeris* (4.1%) as the only putative pathogens after 145 min of overall laboratory analyses and 5 min of bioinformatics analyses (Table 5). Notably, the sequencing process was suboptimal because of the small amount of DNA obtained, which resulted in <20% of pores effectively used at termination of this run. Sanger sequencing from four subsamples revealed *T. cucumeris* (all four subsamples) and Pyronemataceae sp. (two subsamples; Ascomycota).

For the ONT2j run, we grew potato plants inoculated with a suspension of *Phytophthora infestans* (Oomycota) and *B. exigua* isolates in growth chamber MLR-351H (Sanyo, Osaka, Japan). Based on visual examination, the plant individuals did not become infected, apart from bearing tiny brown spots on leaves (sample KL038). The leaf samples were disrupted in liquid N_2 instead of bead beating. The analysis revealed *L. esculentum* (76.6%), *Escherichia coli* (5.4%), *Shigella* sp. (1.2%) and *Salmonella enterica* (0.3%) (all *Bacteria*) and *P. infestans* (0.015%) at low relative abundance. However, Sanger sequencing revealed the presence of both *P. infestans* and *B. exigua*. Because of

TABLE 5 Details of the rapid pathogen diagnostics experiments using the MinION instrument[c]

Sample/run (min)	DNA extraction method[a] (min)	DNA purification (min)	No. of raw/passed reads	Bioinformatics: no. of quality-filtered reads (min)	Pathogen identification (% of sequences)	Total analysis time (min)
KL037/ONT2i (50)	BB, Phire lysis (15)	FavorPrep (25)	1,142/436	97 (40)	*Thanatephorus cucumeris* (4.1)	150
KL038/ONT2j (5)	LN, Phire lysis (40)	FavorPrep (60)	20,000/9,974	6,750 (409)	*Phytophthora infestans* (0.015)	434
KL039/ONT2k (30)	LN, Phire lysis (40)	FavorPrep (55)	5,044/4,046	849 (79)	*Fusarium* aff. *fujikuroi* (0.12)	224
KL040/ONT2l (5)	LN, Phire lysis (35)	FavorPrep (55)	2,000/1,420	669 (132)	*Albugo laibachii* (0.2)	247
KL040/ONT2m (60)	LN, Phire lysis (35)	FavorPrep (55), AMPure (30)	1,074/223	104 (10)	None	ND[b]
KL041/ONT2n (4)	LN, $(NH_4)_2SO_4$ lysis (20)	FavorPrep (20), AMPure (30)	4,000/2,457	1,236 (97)	*Rhizoctonia solani* (2.0)	191

[a]Abbreviations: BB, bead beating; LN, liquid N_2.
[b]ND, not determined because AMPure purification was performed on a subsequent day.
[c]The time used for library preparation and data interpretation took 15 min and 5 min, respectively.

contamination and marginal abundance of one of the two inoculated pathogens, we consider this MinION run unsuccessful.

The ONT2k run of wilted cucumber (*Cucumis sativus* L.) roots (sample KL039) was dominated by *L. esculentum*, a contaminant from the previous run (43.9%), followed by *C. sativus* (11.9%) and *C. melo* (11.8%). Apart from the pathogen *Fusarium* aff. *fujikuroi* (0.12%), the microbiome was dominated by bacteria *Rhodanobacter denitrificans* (3.8%) and *Pseudomonas* aff. *umsongensis* (1.6%), all of which were undetected in the previous run. Sanger sequencing failed because of unreadable chromatograms. Given the lethal effect on plants and low proportion of the pathogen but also a high level of contamination from the previous run, it remains unclear if fusariosis caused wilting.

A diseased *Cucumis sativus* leaf with white powdery infection (sample KL040) was used for the ONT2l run. Rapid analysis of the first 2,000 sequences revealed that *C. sativus* (58.7%) and *C. melo* (27.5%) dominate, but only a single putative pathogen, *Albugo laibachii* (Oomycota), is present (0.2%). Analysis of 20,000 subsequent sequences revealed similar results, with *A. laibachii* contributing 0.07% of sequences. However, Sanger sequencing of the same sample revealed *Peronospora violae* (Oomycota) instead, along with an unidentified mite (*Acari*). Because genomes of *Peronospora* species are unavailable, it is likely that the metagenomic matches to *A. laibachii* actually represent *P. violae*.

For the ONT2m run, the DNA of sample KL040 was further purified using AMPure XP beads. In this run, we had an issue with flow cell loading that resulted in very low accumulation of sequences, which may be attributable to the fourth use of the flow cell. Bioinformatics analysis revealed *C. sativus* (40.4%) and *C. melo* (34.6%) but no putative pathogens among the 104 quality-filtered sequences.

For the ONT2n run, a diseased *S. tuberosum* stem sample was powderized in liquid N_2 and DNA was extracted using $(NH_4)_2SO_4$ lysis, followed by double purification with FavorPrep and AMPure XP beads to rule out the possibility that the latter procedure inhibited the last run. On a new flow cell, sequences accumulated rapidly, revealing *S. esculentum* (75.4%), a *Pseudomonas* sp. (16.7%), and the putative pathogen *T. cucumeris* (2.0%), which matched the symptoms.

We also intended to analyze several infected samples of pine needles, but the protocols used here and in other commercial kits recovered too low a DNA concentration (<5 ng μl^{-1}). Therefore, we decided not to sequence these samples.

DISCUSSION

Use of third-generation sequencing instruments for DNA metabarcoding. Using the same amplicon pools and additional morphology-based or molecular diagnosis, we had a unique opportunity to evaluate the relative performance and biases of MinION compared with Sequel for taxonomic identification. These instruments revealed contrasting results in metabarcoding of Pinaceae species and *S. tuberosum* samples. The results of Sequel were generally consistent with morphology-based and species-specific oligonucleotide PCR-based diagnosis (Pinaceae species samples) and Sanger sequencing results (*S. tuberosum* samples) but failed to distinguish the closely related needle pathogens *D. pini* and *D. septosporum*. This was resolved when sequences were reclustered at 99% sequence similarity. Apart from the species of *Coniothyrium* contaminating the MinION data sets, the two platforms revealed different taxa (by names and INSD accession numbers) prevailing in the same samples. Mostly these MOTUs correspond to closely related sister taxa that share the UNITE Species Hypothesis at 2% distance level, as confirmed by manual comparisons of best-matching reads.

Our MinION runs utilizing washed, reused flow cells, and the same indexed primers suffered from carryover of 13 to 44% of reads originating from a previous run. Furthermore, we could recover traces of a positive control used in the next-to-previous run at 0.2% relative abundance. In MinION flow cells, a sequence carryover rate of 6% has been reported (40). Notably, such carryover contamination is not unique to nanopore technology, as it also occurs in reusable chips of the Ion Torrent platform (41).

In our analyses, MinION had an issue of contamination with a fungal MOTU matching a *Coniothyrium* sp. that was not observed in Sequel runs, negative controls, and our previous data sets. This contamination occurred in two R9.4 flow cells (1 and 2) supplied as a single batch with the MinION instrument but not in other R9.4 batches (flow cells 3, 4, and 5) or the R9.5 batch. Flow cells 1 and 2 were used over 6 months, rendering several independent laboratory contamination events unlikely. Therefore, we suspect that this contamination was inadvertently introduced during manufacture.

Chimeric reads were common in both Sequel and MinION data. UCHIME effectively detected chimeric molecules in the Sequel data, but it performed poorly on the MinION data. We speculate that the error-rich MinION reads were too different from each other to be recognized as chimeric using the algorithm parameters. In contrast to Sequel, a large proportion of long MinION reads represented self-chimeras that were not recognized by UCHIME. In addition, the MinION data included a substantial proportion of chimeric molecules with parents from different samples, representing a unique hybrid issue of index switching and chimera formation that could be detected only manually. This may be related to the formation of chimeric molecules during the library preparation or artifacts of sequencing when molecules pass through nanopores. Since MinION reads are typically mapped to the reference, we estimate that the abundant chimeric molecules create virtually no bias, except for those with switched indexes.

Index switches during library preparation or sequencing make a strong and perhaps predominant contribution to sample contamination (42). The observed index switching rate of 3.6 to 3.8% in MinION compares poorly with that of Sequel ($<$0.2% in this study) and various Illumina instruments (0.1 to 10%) (43). Here, double-size indexes performed equally poorly, suggesting that index switches are attributable to processes in library preparation or sequencing artifacts rather than sequencing errors. In particular, the high rate of index switching spilled the dominant MOTUs in the deeply sequenced MinION data sets across nearly all samples. This partly contributed to the 2-fold- to 4-fold-greater richness per sample compared with the Sequel data sets. The high error rate and inaccurate mapping-based method of MOTU construction certainly add to this difference. Conversely, the clustering of Sequel data at 98% sequence similarity may have been too conservative, because many putative plant-pathogenic fungal species differ from each other by only a few bases in the ITS region (e.g., the Pinaceae-specific needle pathogens *D. pini* and *D. septosporum*) (44); therefore, several species with distinct ecology and pathology may be lumped into a single taxon (45). Reanalysis of Sequel sequence data indicated that these species can be successfully separated at 99% sequence similarity (not shown). In spite of substantial disparity in the taxon-rich ITS1catta-ITS4ngsUni data subsets, the two instruments revealed a great overlap in the species-poor ITS1Oo-ITS4ngsUni data subset.

The average error rate of MinION reads was 10 to 15%, depending on the proportion of homopolymers in the marker gene region of particular species. MOTUs possessing homopolymer-rich ITS markers were up to 2 orders of magnitude less common in the MinION (ONT2) than in the Sequel (Sequel2) run. This is supported by the observation that these MOTUs were relatively more common in the failed bin than other MOTUs. In particular, the most homopolymer-rich positive-control sample was 16-fold more common in the failed bin than expected. Possibilities to solve this include lowering the initial quality threshold (Phred score) or including the failed reads in analyses.

We observed discrimination against longer reads when sequencing potato amplicons using the $1D^2$ approach (ONT2f), which confirms a previous report (40). Preferential recovery of shorter reads seems to be inherent to both PCR and all sequencing instruments, including Sequel (6, 7, 12).

Rapid molecular diagnostics. We tested both metagenomics- and amplicon-based approaches of MinION sequencing for rapid identification of pathogens. Most taxa recovered in the metagenome run were rare in the amplicon data set and vice versa. Although we detected severe biases in MinION amplicon sequencing, we believe that amplicon-based analyses are more accurate than metagenomics analyses and that

reference bias accounts for much of the difference; i.e., in metagenomics analyses, species with available reference genomes have a much greater chance of accumulating hits than species with no available genomes. In our analyses, this is illustrated by misidentification of a potato as a tomato. Mapping reads of an ascomycete pathogen to genomes of several others, as in our study, is likely to remain cryptic. A solution may be sufficiently deep metagenomics sequencing to secure coverage of mitochondrial or ITS markers that occur in multiple copies per genome. Because most bacterial and fungal human pathogens have available genome sequences, nanopore metagenomics-based identification may be better suited to medical samples, but this situation is likely to improve very soon in plant pathology.

In spite of multiple quality issues in MinION runs, we demonstrate that accurate molecular identification from sample collection through DNA extraction, concentration, library preparation, sequencing, bioinformatics, and taxonomic interpretation takes as little as 2.5 h using nanopore sequencing in the metagenome mode (Fig. 3). With no specific DNA extraction step, identification of bacterial human pathogens from urine was performed in 4 h (36). Multiple other studies report on running the full analysis work flow in 1 day (22, 37, 46). When accounting for all technological advances in molecular and bioinformatics analyses, the nanopore analysis work flow for plant and animal tissues potentially can be reduced to $<$2 h for metagenomes and ca. 3 h for amplicons (Fig. 3). However, it requires (i) that the DNA is easily extractable in high quantity and purity (47), (ii) amplification is performed by methods alternative to those of conventional slow polymerases (48), (iii) nanopore library preparation follows methods for rapid library kits, and (iv) the sequencing process is limited to ca. 15 min after obtaining a critical number of reads (37). These express diagnostics rates of MinION cannot be beaten by instruments of other HTS platforms that require several hours for library preparation and at least 1 day for sequencing (49).

However, there is a clear trade-off between overall analysis time and data reliability in MinION sequencing. Shortened DNA extraction protocols may yield lower quality and quantity of DNA, whereas culled incubation and centrifugation steps in library preparation may result in dilute and poorly indexed libraries overrepresented by short fragments. Although we successfully identified microorganisms from *S. tuberosum* using a library 13-fold more dilute than recommended, it may be useful to add a certain amount of so-called carrier DNA to secure preparation of high-quality libraries (50). We anticipate that sample preparation, bioinformatics, and interpretation processes take longer for multiplexed samples, which may be necessary to reduce the overall analytical costs per sample by an order of magnitude when using Oxford Nanopore's commercial multiplexing kits or by 3 orders of magnitude by applying custom multiplexing methods of indexed primers (51). To reduce the chances of carryover of previous molecules, contamination-aware indexes, i.e., different indexes across runs (e.g., runs ONT2 and ONT2a in this study), could be used.

Technical and analytical issues. Although several authors have reported species-level identification of bacterial taxa in complex communities using MinION (35, 52), these interpretations are not convincing, because mapping of sequences with 10 to 25% errors to reference reads of high similarity is inaccurate (described above). We demonstrate that even when using the relatively rapidly evolving fungal ITS region and reference sequences differing from each other by at least 2%, positive-control samples and plant material yield multiple MOTUs, sometimes recovering strongest hits to different species or genera. Conversely, species absent from databases may be mapped to one or more closely related species, which may provide incorrect taxonomic implications. This is of particular importance in molecular diagnostics, necessitating inclusion of marker genes of all potential target species in the reference database to prevent incorrect interpretation. The metagenomics approach requires a comprehensive database of genomes of all potential target organisms, which strongly depends on whole-genome sequencing initiatives. Exome compilations are suboptimal, because much of the eukaryotic DNA is noncoding. Besides target organisms, metagenomics databases

also require inclusion of specific interacting taxa (e.g., *S. tuberosum*), contaminants (*Homo sapiens* and species propagated in laboratories), and various bacteria that contribute much to the metagenomic DNA.

A major concern with novel sequencing techniques is the paucity of reports on analytical shortfalls and the nature of artifacts, which may partly be derived from the lack of controls or inappropriate sampling design (53). The MinION instrument has been used for 5 years, but so far there is limited information about analytical errors and biases, and a few authors mention checking chimeras, index-switching artifacts, or unsuccessful runs (however, see references 40, 54, and 55). It is important to raise the awareness of the scientific community about the limitations and potential issues when choosing among analytical methods and interpreting data.

Perspectives of third-generation sequencing technologies. Both Oxford Nanopore and PacBio sequencing platforms are rapidly evolving in terms of read length and base-calling accuracy. At the moment, Sequel seems to be the best choice for metabarcoding of regular-size (600 to 1,000 bp) and long (up to 4.5 kb) amplicons (6, 7, 12, 56–58) and for barcoding using ultralong markers (up to 7 kb) (59). The recently released M8 chemistry has reduced the per read cost of PacBio sequencing roughly threefold. Declining costs and greater throughput, read length, and quality continue to promote Sequel for metabarcoding, metagenomics, and metatranscriptomics (https://www.pacb.com/videos/webinar-sequence-with-confidence-introducing-the-sequel-ii-system/). Although Sequel enables reliable separation of species at 99% sequence similarity based on the full-length ITS region, it may be hard to convince users of Illumina MiSeq to switch to another platform and adopt alternative bioinformatics work flows.

Use of MinION for metabarcoding offers little promise considering the current state-of-the-art technology, with unacceptably high error rates. The error rates should be reduced to $<$0.1%, i.e., to the level of Illumina instruments and circular consensus of Sequel for use in routine biodiversity assessments. Several methods of tandem repeat (concatemer) sequencing enable the reduction of error rates to 1 to 3% (27–29). Double barcoding of each size-selected RNA or DNA molecule followed by generation of consensus sequences yields quality improvements comparable to tandem repeat sequencing (60), but it would require ultrahigh sequencing depth to reach a 1% error rate and to be able to multiplex over several biological samples. Combining these methods may facilitate reducing error rates toward the critical threshold but also adds to time and cost of analysis.

For regular barcoding, the third-generation sequencing tools offer great promise in situations where their throughput and read length are much superior to double-pass Sanger sequencing, i.e., for barcodes of $>$1,000 bases and multiplexing hundreds of samples to secure cost efficiency (16, 51). Sanger sequencing handles poorly the alleles or copies of markers with read length polymorphism, which is common in noncoding regions of eukaryotes. The third-generation HTS technologies are able to recover various alleles as well as pseudogenes (26) from mixed or contaminated samples by sequencing single DNA molecules. Both Sequel and MinION are capable of handling DNA amplicons of $>$7,000 bases, requiring generation of consensus reads for reliable results (59). Although we could reach up to 99.5% accuracy with $>$100 MinION reads, 100 reads were considered sufficient for generating principally error-free barcodes for animals using the $1D^2$ approach (30). For PacBio instruments, a single read may be enough for reads of around 2,000 bases, but three or more may be needed for longer fragments and to average over PCR errors (58).

Unlike Sequel and other HTS technologies, MinION is well suited to rapid diagnostics of pathogens and invasive species, especially in groups that are well-known and well referenced in public sequence databases. Besides detection of pathogenic species, MinION has the potential to recover antibiotic resistance genes and pathogenesis-related genes as well as single mutations in the metagenomics mode (26, 61). By using multiplex amplicons or a metagenomics/genomics approach, it will be possible to

detect harmful organisms and their specific pathogenicity-related genomic features in less than 1 day (36). Besides enabling users to trace taxon/gene exchange between different habitats (62), this approach has important implications for improving diagnosis and implementing countermeasures, e.g., releasing biocontrol agents, spraying biocides, or arranging quarantine.

Nanopore-based detection methods are flexible for incorporating additional options, such as recording epigenetic modifications (11, 63) and primary structure of RNA (64), proteins (65), and polysaccharides (66). Alternative nanopore-based DNA sequencing methods are also evolving (67). The potential of different nanopores to record various biomolecules indicates great promise of nanopore-based molecular diagnostics in the future.

Conclusions. We demonstrate that the MinION device is well suited for rapid PCR-free diagnosis of fungal and oomycete pathogens and other eukaryotic organisms, which may take as little as 150 min from sample preparation (including DNA extraction, library preparation, sequencing, and bioinformatics) to data interpretation. However, care should be taken to secure profound reference sequence data to avoid misdiagnosis. Amplicon-based diagnostics take longer but are more accurate if genomes of potential pathogens, hosts, or other associated organisms are unavailable. For whole-community metabarcoding, Sequel performs much better than MinION in terms of data quality and analytical biases. Although tandem repeat sequencing and read consensus sequencing have been developed for MinION, their error rate of 1 to 3% is still insufficient for exploratory metabarcoding analyses of biodiversity, but this may change in the coming years.

MATERIALS AND METHODS

Sample preparation. The *S. tuberosum* subset includes 27 samples of leaves and 10 samples of tubers with symptoms of disease (Table 6). We also included a DNA sample of two Australian Tuberaceae (Ascomycota) species as a positive control. The Pinaceae species subset includes 36 distinct needle samples from eight species of *Pinus* and two species of *Picea* that represent material with symptoms of needle blight or no symptoms. The foliar samples of natural, planted, or recently imported trees were collected in Estonia in 2011 to 2018 (Table 7). We included a cultured isolate of *D. pini* (146889), *D. septosporum* (150931), and the closely related *Lecanosticta acicola* (150943; all Ascomycota) as positive controls. Unequal mixtures of DNA from these cultures served as a simple mock community. In both subsets, we included a negative-control sample.

In Pinaceae species samples, DNA from 0.2 g plant material and fungal cultures was extracted using the GeneJET genomic DNA purification kit (Thermo Fisher Scientific, Waltham, MA, USA). In *S. tuberosum* samples, DNA from 0.1 g diseased fresh leaf tissue was extracted using a lysis buffer [0.8 M Tris-HCl, 0.2 M $(NH_4)_2SO_4$, 0.2% (wt/vol) Tween 20; Solis BioDyne, Tartu, Estonia].

Molecular identification. Pinaceae species samples were screened for specific pathogenic fungi *Dothiostroma pini*, *D. septosporum*, and *Lecanosticta acicola* using species-specific primer pairs by following the developer's protocols (68). Samples from potato and cultured needle fungi were amplified using the ITS1F + ITS4 primer pair for Fungi (69, 70). The potato samples were also amplified for oomycetes using the ITS1Oo + ITS4 primer pair (71, 72). For sequencing of fungi and oomycetes, ITS5 (69) and ITS1Oo primers, respectively, were used. Some amplicons were resequenced using primers ITS2, ITS3, and ITS4 (69).

For the metabarcoding approach, we used forward primer ITS1catta (5′-ACCWGCGGARGGATCATT A-3′) (73) and reverse primer ITS4ngsUni (74) to be able to selectively amplify fungal DNA and simultaneously avoid the 18S rRNA gene intron bias. Located in the terminus of the 18S rRNA gene, the ITS1catta primer covers nearly all Ascomycota and Basidiomycota as well as selected groups of zygomycetes and early diverging lineages but discriminates against plants and most other eukaryote groups (including fungal taxa Mortierellomycota and Tulasnellaceae) in the last 3′ position. For Oomycota, we used the ITS1Oo primer in combination with the ITS4ngsUni primer for the potato data set in parallel. Forward primers were tagged with one of the 12-base Golay indexes with at least four differences from any other index (12). Because of issues in data recovery, we also amplified a subset of eight *S. tuberosum* samples (KL001 to KL008) using ITS1catta and ITS4ngsUni primers in which the forward primer was equipped with a tandem repeat barcode of double length (securing at least an 8-base difference) to increase resolution among samples. Because the $1D^2$ nanopore sequencing method requires DNA fragments of >3 kb, we amplified these *S. tuberosum* samples (roughly 3.2-kb amplicons) using the indexed ITS1catta primer combined with the LR14 primer (75). For comparing the metabarcoding approach to the metagenomics method, we used ITS1catta in combination with the LR11 primer (75), which yielded stronger amplicons than LR14. We used negative and positive controls as described above.

PCR was performed in a 25-μl volume comprising 0.5 μl each of the tagged primer (20 μM), 5 μl HOT FIREPol blend master mix (Solis Biodyne), 1 μl DNA extract, and 18 μl double-distilled H_2O. Thermocycling conditions included an initial 15-min denaturation at 95°C, 30 cycles of 30 s of denaturation, 30 s of annealing

TABLE 6 Details of needle samples collected in Estonia

Sample ID	Collection locality	Collection date (day.mo.yr)	Host	Substrate[b]	Disease symptom
115	Tallinn Botanic Garden	17.11.2011	*Pinus sylvestris*	Needle	*Dothistroma*-like
117	Tallinn Botanic Garden	17.11.2011	*P. sylvestris*	Needle	*Dothistroma*-like
118	Pirita	17.11.2011	*P. mugo*	Needle	*Dothistroma*-like
119	Tallinn Botanic Garden	17.11.2011	*P. sylvestris*	Needle	*Dothistroma*-like
123	Tallinn Botanic Garden	17.11.2011	*P. uncinata*	Needle	*Dothistroma*-like
125	Tallinn Botanic Garden	17.11.2011	*P. rigida*	Needle	*Dothistroma*-like
127	Tallinn Botanic Garden	17.11.2011	*P. contorta*	Needle	*Dothistroma*-like
139	Tallinn Botanic Garden	15.08.2011	*P. x rotundata*	Needle	*Dothistroma*-like
141	Tallinn Botanic Garden	15.08.2011	*P. mugo*	Needle	*Dothistroma*-like
142	Tallinn Botanic Garden	15.08.2011	*P. x rotundata*	Needle	*Dothistroma*-like
148	Tallinn Botanic Garden	15.09.2011	*P. mugo* var. *pumilio*	Needle	*Dothistroma*-like
154	Tallinn Botanic Garden	15.09.2011	*P. rhaetica*	Needle	*Dothistroma*-like
2404	Petrivka, The Ukraine	10.09.2013	*P. nigra* subsp. *pallasiana*	Living culture: DoPi	NA
3904	Kärevere	20.01.2015	*P. mugo*	Living culture: LeAc	NA
3906	Kärevere	20.01.2015	*P. mugo*	Living culture: DoSe	NA
4154	NA[a]	09.10.2014	NA	Mock: DoPi, DoSe, LeAc	NA
4162	Levala	09.10.2014	*P. sylvestris*	Needle	*Dothistroma*-like
4180	Kolli	13.10.2014	*P. sylvestris*	Needle	*Dothistroma*-like
4181	Mustumetsa	13.10.2014	*P. sylvestris*	Needle	*Dothistroma*-like
4192	Soohara	07.10.2014	*P. sylvestris*	Needle	*Dothistroma*-like
4194	Värska	07.10.2014	*P. sylvestris*	Needle	*Dothistroma*-like
4195	Vastse-Kuuste	07.10.2014	*P. mugo*	Needle	*Dothistroma*-like
4197	Partsi	07.10.2014	*P. sylvestris*	Needle	*Dothistroma*-like
4220	Sääre	15.10.2014	*P. sylvestris*	Needle	*Dothistroma*-like
4221	Unimäe	15.10.2014	*P. sylvestris*	Needle	*Dothistroma*-like
4222	Tori	16.10.2014	*P. mugo*	Needle	*Dothistroma*-like
4223	Tori	16.10.2014	*P. mugo*	Needle	*Dothistroma*-like
5136	Imported: Netherlands	03.11.2015	*P. mugo* var. *pumilio*	Needle	Asymptomatic
5137	Imported: Netherlands	17.12.2015	*Picea omorika*	Needle	Asymptomatic
5146	Imported: Netherlands	03.11.2015	*P. mugo*	Needle	Asymptomatic
5148	Imported: Netherlands	03.11.2015	*P. mugo*	Needle	Asymptomatic
5151	Imported: Netherlands	03.11.2015	*P. sylvestris*	Needle	Asymptomatic
5186	Imported: Netherlands	26.10.2015	*P. peuce*	Needle	Asymptomatic
5194	Imported: Netherlands	26.10.2015	*P. koraiensis*	Needle	Asymptomatic
5195	Imported: Netherlands	26.10.2015	*P. mugo*	Needle	Asymptomatic
5297	Imported: Germany	17.12.2015	*Picea pungens*	Needle	Asymptomatic
5307	Imported: Germany	17.12.2015	*Picea omorika*	Needle	Asymptomatic
14374	Agali	16.02.2018	*P. sylvestris*	Needle	*Lecanosticta*-like
14378	Agali	16.02.2018	*P. mugo*	Needle	*Lecanosticta*-like

[a]NA, not applicable.
[b]Abbreviations for species: DoPi, *Dothiostroma pini*; DoSe, *D. septosporum*; LeAc, *Lecanosticta acicola*.

at 55°C, and 60 s of elongation at 72°C, with a final 10-min elongation before hold at 4°C. The number of cycles was increased to 35 or 38 for some samples to yield a visible amplicon on 1% agarose gel. For the ITS1Oo + ITS4ngsUni primer combination, 40 PCR cycles at 50°C annealing were used to secure greater product recovery. The two replicate amplicons were pooled, checked on a gel, and mixed with amplicons of other samples in roughly equal proportions based on visual estimates of band size.

Third-generation sequencing. The mixed amplicons of *S. tuberosum* and those of Pinaceae species needles were separately split into library preparation for Sequel and MinION. The two PacBio libraries were sequenced on a Sequel instrument using the same SMRT cell (SMRT cell 1M, v2, Sequel Polymerase v2.1, sequencing chemistry v2.1, loading by diffusion, movie time of 600 min, preextension time of 30 min). The PacBio CCS reads (minPasses = 3, MinAccuracy = 0.9) were generated using SMRT Link v 6.0.0.47841 (Pacific Biosciences). Subsequent bioinformatics were performed using PipeCraft 1.0 (76), which included steps of demultiplexing (2 mismatches to primer and 1 mismatch to tag), extraction of the ITS region (ITSx: default options) (77), chimera removal (UCHIME: *de novo* and reference-based methods combined) (78), additional filtering option "remove primer artifacts," which removes chimeric sequences where the full-length primer is found somewhere in the middle of the read, clustering (UPARSE: 98% sequence similarity threshold) (79), and taxonomic identification (BLASTn: E value = 0.001, word size = 7, reward = 1, penalty = −1, gap open = 1, gap extend = 2;) (80) against the UNITE 7.2 (45) reference database. We used the criteria of a BLAST E value of $<e^{-40}$ and sequence similarity of >75% for the kingdom-level identification and E value of $<e^{-50}$ for phylum- and class-level identification.

For the MinION instrument, amplicon library preparation was performed using the 1D amplicon/cDNA by a ligation (SQK-LSK109) kit (ONT) using R9.4 flow cells by following the manufacturer's instructions. For long fragments, we also used the $1D^2$ sequencing of genomic DNA (SQK-LSK308) kit on an R9.5 flow cell by following the producer's protocols (run ONT2f). Flow cells were used 1 to 3 times,

TABLE 7 Details of *S. tuberosum* and *C. sativa* samples collected in Estonia

Sample ID	Collection locality	Collection date (day.mo.yr)	Cultivar[a]	Substrate	Disease symptom[b]
KL001	Õssu	02.08.2017	St Ants	Leaf	DCL
KL002	Õssu	02.08.2017	St Ants	Leaf	DCL
KL003	Õssu	02.08.2017	St Ants	Leaf	DCL
KL004	Õssu	02.08.2017	St Ants	Leaf	DCL
KL005	Õssu	02.08.2017	St Sarpo Mira	Leaf	DCL
KL006	Õssu	02.08.2017	St Sarpo Mira	Leaf	DCL
KL007	Õssu	02.08.2017	St Sarpo Mira	Leaf	DCL
KL008	Õssu	02.08.2017	St Sarpo Mira	Leaf	DCL
KL009	Õssu	02.08.2017	St Toluca	Leaf	DCL
KL010	Õssu	02.08.2017	St Toluca	Leaf	DCL
KL011	Õssu	02.08.2017	St Toluca	Leaf	DCL
KL012	Õssu	02.08.2017	St Toluca	Leaf	DCL
KL013	Õssu	02.08.2017	St Toluca	Leaf	DCL
KL014	Õssu	02.08.2017	St Toluca	Leaf	DCL
KL015	Õssu	02.08.2017	St Toluca	Leaf	DCL
KL016	Õssu	02.08.2017	St Toluca	Leaf	DCL
KL017	Õssu	02.08.2017	St Kelly	Leaf	DCL
KL018	Õssu	02.08.2017	St Kelly	Leaf	DCL
KL019	Õssu	02.08.2017	St Kelly	Leaf	DCL
KL020	Õssu	02.08.2017	St Kelly	Leaf	DCL
KL021	Karala	02.08.2017	St unknown	Leaf	DCL
KL022	Karala	02.08.2017	St unknown	Leaf	DCL
KL023	Karala	02.08.2017	St unknown	Leaf	DCL
KL024	Karala	02.08.2017	St unknown	Leaf	DCL
KL025	Metsaküla	12.08.2017	St unknown	Leaf	DCL
KL026	Metsaküla	12.08.2017	St unknown	Leaf	DCL
KL027	Metsaküla	12.08.2017	St unknown	Leaf	DCL
KL028	Väljataguse	11.04.2018	St Elfe	Tuber	Potato gangrene
KL029	Väljataguse	11.04.2018	St Elfe	Tuber	Potato gangrene
KL030	Väljataguse	11.04.2018	St Elfe	Tuber	Potato gangrene
KL031	Õssu	11.04.2018	St Laura	Tuber	Potato gangrene
KL032	Suur-Rahula	11.04.2018	St Gala	Tuber	Potato gangrene
KL033	Tagaküla	11.04.2018	St Laura	Tuber	Potato gangrene
KL034	Tagaküla	11.04.2018	St Laura	Tuber	Potato gangrene
KL035	Padise	11.04.2018	St Marabel	Tuber	Potato gangrene
KL036[c]	Õssu	30.08.2018	St Carolus	Tuber	*Rhizoctonia*-like
KL037[d]	Õssu	30.08.2018	St Carolus	Tuber	*Rhizoctonia*-like
KL038[d]	Tartu	16.05.2019	St Carolus	Leaf	DCL
KL039[d]	Eistvere	20.05.2019	Cs Carambole	Roots	Wilted
KL040[d]	Luunja	22.05.2019	Cs Petrifin	Leaf	White powdery spots
KL041[d]	Roiu	30.05.2019	St Flavia	Stem	*Rhizoctonia*-like

[a]St, *Solanum tuberosum*; Cs, *Cucumis sativa*.
[b]DCL, dark circular lesions.
[c]Used only for the ONT2g and ONT2h runs.
[d]Used only for the rapid identification run.

being cleaned once or twice using the wash kit (EXP-WSH002; ONT). Sequencing was performed in the laboratory at room temperature, connecting the MinION device to a plugged-in, Internet-connected laptop computer with four processors and 32 GB RAM. For base calling in MinKnow 3.1.19 software (ONT), we used the default Phred score of 11, which placed the reads into passed and failed bins. The passed FASTA-formatted reads (additionally failed reads in runs ONT2g and ONT2h) were further subjected to bioinformatics analysis using PipeCraft. The options in PipeCraft included demultiplexing of metabarcoding reads allowing no mismatches to the barcode, followed by BLASTn search using default settings. The sequencing adaptors were removed by a custom script.

Given the poor overall sequence quality, traditional MOTU-based approaches are not applicable to the MinION data; therefore, we mapped reads based on their best matches to database sequences in the UNITE reference database by following the principles of previous nanopore sequencing studies (33, 35). Limitations of this approach are outlined in Discussion.

The rate of index switching was calculated based on the average of the distribution of MOTUs corresponding to the positive-control sample in experimental samples and the distribution of other MOTUs in the positive-control sample relative to the overall amount of sequences in positive-control samples (12). It assumes that reads belonging to different MOTUs and samples exhibit equal probability of switching indexes. We also assessed potential index switching in the putatively chimeric sequences by manual BLAST searches of these sequences against the INSD by following Hyde et al. (4). Chimeric reads that had one part belonging to a parent not found in the particular sample were considered cross-sample chimeras.

To evaluate the relative efficiency of metagenomics approaches on pathogen recovery, we used DNA from the *S. tuberosum* tuber sample KL036 (run ONT2g compared to the amplicon run ONT2h from the same sample) (Table 1). For library preparation, the rapid sequencing kit (SQK-RAD004; ONT) was used by following the manufacturer's instructions. Base calling was performed as described above. Both passed and failed sequences were used in further bioinformatics analyses as implemented in PipeCraft. We relied on the entire INSD as a metagenomics reference database.

Rapid pathogen diagnostics. We further elaborated on the metagenomics approach to maximize the speed of pathogen diagnosis using the MinION instrument. For ONT2i, ONT2j, ONT2k, ONT2l, ONT2m, and ONT2n runs (Table 1), we used ca. 20 mg of infected tissue of *S. tuberosum* or *Cucumis sativa* samples and optimized rapid extraction protocols (Table 5). We used ca. 20 mg fresh material for extraction in two technical replicates in 2-ml Eppendorf tubes that contained either 100 μl Phire plant direct PCR kit lysis buffer (Thermo Fisher Scentific) or 500 μl $(NH_4)_2SO_4$-based lysis buffer [0.8 M Tris-HCl, 0.2 M $(NH_4)_2SO_4$, 0.2% (wt/vol) Tween 20; Solis BioDyne]. The Phire lysis protocol was shortened by reducing the step of lysis to 2 to 5 min, preceded by tissue disruption using bead beating (5 min at 30 Hz) or a mortar and pestle in liquid N_2, followed by brief centrifugation at 5,000 $\times$ *g*, incubation at 30°C for 5 min, and a final centrifugation at 11,000 $\times$ *g* for 1 min. The $(NH_4)_2SO_4$ lysis included incubation time reduced to 5 min, followed by incubation at 98°C for 2 min. The DNA was concentrated from lysate using the FavorPrep gel/PCR purification kit (Favorgen Biotech Corp., Vienna, Austria) by following the manufacturer's instructions, except including centrifugation steps for 1 min and final elution using 50 μl water. Some samples were further subjected to Agencourt AMPure XP bead purification (Beckman Coulter, East Windsor, NJ, USA) to remove DNA fragments of <500 bases. DNA concentration was measured using QUBIT. For library preparation, we used the SQK-RAD004 kit and followed the manufacturer's protocols, except with shortened fragmentation time at 30°C of 30 s. MinION runs were performed on R9.4 flow cells, and the data were downloaded after obtaining sufficient amounts of sequences (Table 5). The runs were interrupted in 1 to 2 h (Table 1). Only the passed sequences were used in further bioinformatics analyses using PipeCraft by following the options for the ONT2g metagenomic run.

Data availability. Sanger sequences of potato samples have been deposited in the UNITE database (https://unite.ut.ee/) and INSD databases (GenBank accession numbers MN065746 to MN065768). Representative Sequel sequences of 99% similarity consensus were generated using PipeCraft and uploaded to the UNITE database, which is the only repository that accepts quality-filtered HTS reads. Raw sequence data of MinION and Sequel are available from the PlutoF digital repository and the Sequence Read Archive (PRJNA545967), respectively. Sample-by-MOTU tables used in these analyses can be accessed from the PlutoF digital repository (https://plutof.ut.ee/#/filerepository/view/3431905).

ACKNOWLEDGMENTS

We thank V. Kisand and three anonymous referees for constructive comments on the manuscript and A. Tooming-Klunderud for running PacBio sequencing.

Financial contribution was provided by the Estonian Science Foundation (grants PUT1399, PUT1317, PSG136, IUT21-04, IUT 36-2, MOBERC13, and ECOLCHANGE).

REFERENCES

1. Comtet T, Sandionigi A, Viard F, Casiraghi M. 2015. DNA (meta)barcoding of biological invasions: a powerful tool to elucidate invasion processes and help managing aliens. Biol Invasions 17:905–922. https://doi.org/10.1007/s10530-015-0854-y.
2. Kashyap PL, Rai P, Kumar S, Chakdar H, Srivastava AK. 2017. DNA barcoding for diagnosis and monitoring of fungal plant pathogens, p 87–122. *In* Singh BP, Gupta VK (ed), Molecular markers in mycology. Springer-Verlag, New York, NY.
3. Grosdidier M, Aguayo J, Marçais B, Ioos R. 2017. Detection of plant pathogens using real-time PCR: how reliable are late Ct values? Plant Pathol 66:359–367. https://doi.org/10.1111/ppa.12591.
4. Hyde KD, Udayanga D, Manamgoda DS, Tedersoo L, Larsson E, Abarenkov K, Bertrand Y, Oxelman B, Hartmann M, Kauserud H, Ryberg M, Kristiansson E, Nilsson RH. 2013. Incorporating molecular data in fungal systematics: a guide for aspiring researchers. Curr Res Environ Appl Microbiol 3:1–32. https://doi.org/10.5943/cream/3/1/1.
5. Bik HM, Porazinska D, Creer S, Caporaso JG, Knight R, Thomas WK. 2012. Sequencing our way towards understanding global eukaryotic biodiversity. Trends Ecol Evol 27:233–243. https://doi.org/10.1016/j.tree.2011.11.010.
6. Nilsson RH, Anslan S, Bahram M, Wurzbacher C, Baldrian P, Tedersoo L. 2019. Mycobiome diversity: high-throughput sequencing and identification of fungi. Nat Rev Microbiol 17:95–109. https://doi.org/10.1038/s41579-018-0116-y.
7. Tedersoo L, Drenkhan R, Anslan S, Morales-Rodriguez C, Cleary M. 2019. High-throughput identification and diagnostics of pathogens and pests: overview and practical recommendations. Mol Ecol Resour 19:47–76. https://doi.org/10.1111/1755-0998.12959.
8. Mosher JJ, Bowman B, Bernberg EL, Shevchenko O, Kan J, Korlach J, Kaplan LA. 2014. Improved performance of the PacBio SMRT technology for 16S rDNA sequencing. J Microbiol Methods 104:59–60. https://doi.org/10.1016/j.mimet.2014.06.012.
9. Schloss PD, Jenior ML, Koumpouras CC, Westcott SL, Highlander SK. 2016. Sequencing 16S rRNA gene fragments using the PacBio SMRT DNA sequencing system. Peer J 4:e1869. https://doi.org/10.7717/peerj.1869.
10. Weirather JL, de Cesare M, Wang Y, Piazza P, Sebastiano V, Wang X-J, Buck D, Au KF. 2017. Comprehensive comparison of Pacific Biosciences and Oxford Nanopore Technologies and their applications to transcriptome analysis. F1000Res 6:100. https://doi.org/10.12688/f1000research.10571.2.
11. Jain M, Koren S, Miga KH, Quick J, Rand AC, Sasani TA, Tyson JR, Beggs AD, Dilthey AT, Fiddes IT, Malla S, Marriott H, Nieto T, O'Grady J, Olsen HE, Pedersen BS, Rhie A, Richardson H, Quinlan AR, Snutch TP, Tee L, Paten B, Phillippy AM, Simpson JT, Loman NJ, Loose M. 2018. Nanopore sequencing and assembly of a human genome with ultra-long reads. Nat Biotechnol 36:338. https://doi.org/10.1038/nbt.4060.
12. Tedersoo L, Tooming-Klunderud A, Anslan S. 2018. PacBio metabarcoding of fungi and other eukaryotes: biases and perspectives. New Phytol 217:1370–1385. https://doi.org/10.1111/nph.14776.
13. Eid J, Fehr A, Gray J, Luong K, Lyle J, Otto G, Peluso P, Rank D, Baybayan P, Bettman B, Bibillo A, Bjornson K, Chaudhuri B, Christians F, Cicero R, Clark S, Dalal R, Dewinter A, Dixon J, Foquet M, Gaertner A, Hardenbol P,

Heiner C, Hester K, Holden D, Kearns G, Kong X, Kuse R, Lacroix Y, Lin S, Lundquist P, Ma C, Marks P, Maxham M, Murphy D, Park I, Pham T, Phillips M, Roy J, Sebra R, Shen G, Sorenson J, Tomaney A, Travers K, Trulson M, Vieceli J, Wegener J, Wu D, Yang A, Zaccarin D, Zhao P, Zhong F, Korlach J, Turner S. 2009. Real-time DNA sequencing from single polymerase molecules. Science 323:133–138. https://doi.org/10.1126/science.1162986.

14. Rhoads A, Au KF. 2015. PacBio sequencing and its applications. Genomics Proteomics Bioinformatics 13:278–289. https://doi.org/10.1016/j.gpb.2015.08.002.
15. Giordano F, Aigrain L, Quail MA, Coupland P, Bonfield JK, Davies RM, Tischler G, Jackson DK, Keane TM, Li J, Yue J-X, Liti G, Durbin R, Ning Z. 2017. *De novo* yeast genome assemblies from MinION, PacBio and MiSeq platforms. Sci Rep 7:3935. https://doi.org/10.1038/s41598-017-03996-z.
16. Hebert PDN, Braukmann TWA, Prosser SWJ, Ratnasingham S, deWaard JR, Ivanova NV, Janzen DH, Hallwachs W, Naik S, Sones JE, Zakharov EV. 2018. A Sequel to Sanger: amplicon sequencing that scales. BMC Genomics 19:219. https://doi.org/10.1186/s12864-018-4611-3.
17. Singer E, Bushnell B, Coleman-Derr D, Bowman B, Bowers RM, Levy A, Gies EA, Cheng J-F, Copeland A, Klenk H-P, Hallam SJ, Hugenholtz P, Tringe SG, Woyke T. 2016. High-resolution phylogenetic microbial community profiling. ISME J 10:2020–2032. https://doi.org/10.1038/ismej.2015.249.
18. Wagner J, Coupland P, Browne HP, Lawley TD, Francis SC, Parkhill J. 2016. Evaluation of PacBio sequencing for full-length bacterial 16S rRNA gene classification. BMC Microbiol 16:274. https://doi.org/10.1186/s12866-016-0891-4.
19. Walder F, Schlaeppi K, Wittwer R, Held AY, Vogelgsang S, van der Heijden MG. 2017. Community profiling of Fusarium in combination with other plant-associated fungi in different crop species using SMRT sequencing. Front Plant Sci 8:2019. https://doi.org/10.3389/fpls.2017.02019.
20. Mikheyev AS, Tin M. 2014. A first look at the Oxford Nanopore MinION sequencer. Mol Ecol Resour 14:1097–1102. https://doi.org/10.1111/1755-0998.12324.
21. Lu H, Giordano F, Ning Z. 2016. Oxford Nanopore MinION sequencing and genome assembly. Genomics Proteomics Bioinformatics 14:265–279. https://doi.org/10.1016/j.gpb.2016.05.004.
22. Quick J, Loman NJ, Duraffour S, Simpson JT, Severi E, Cowley L, Bore JA, Koundouno R, Dudas G, Mikhail A, Ouédraogo N, Afrough B, Bah A, Baum JHJ, Becker-Ziaja B, Boettcher JP, Cabeza-Cabrerizo M, Camino-Sánchez Á, Carter LL, Doerrbecker J, Enkirch T, Dorival IG, Hetzelt N, Hinzmann J, Holm T, Kafetzopoulou LE, Koropogui M, Kosgey A, Kuisma E, Logue CH, Mazzarelli A, Meisel S, Mertens M, Michel J, Ngabo D, Nitzsche K, Pallasch E, Patrono LV, Portmann J, Repits JG, Rickett NY, Sachse A, Singethan K, Vitoriano I, Yemanaberhan RL, Zekeng EG, Racine T, Bello A, Sall AA, Faye O, Faye O, Magassouba N, Williams CV, Amburgey V, Winona L, Davis E, Gerlach J, Washington F, Monteil V, Jourdain M, Bererd M, Camara A, Somlare H, Camara A, Gerard M, Bado G, Baillet B, Delaune D, Nebie KY, Diarra A, Savane Y, Pallawo RB, Gutierrez GJ, Milhano N, Roger I, Williams CJ, Yattara F, Lewandowski K, Taylor J, Rachwal P, J Turner D, Pollakis G, Hiscox JA, Matthews DA, Shea MKO, Johnston AM, Wilson D, Hutley E, Smit E, Di Caro A, Wölfel R, Stoecker K, Fleischmann E, Gabriel M, Weller SA, Koivogui L, Diallo B, Keïta S, Rambaut A, Formenty P, Günther S, Carroll MW. 2016. Real-time, portable genome sequencing for Ebola surveillance. Nature 530:228–232. https://doi.org/10.1038/nature16996.
23. Johnson SS, Zaikova E, Goerlitz DS, Bai Y, Tighe SW. 2017. Real-time DNA sequencing in the Antarctic dry valleys using the Oxford Nanopore sequencer. J Biomol Tech 28:2. https://doi.org/10.7171/jbt.17-2801-009.
24. Castro-Wallace SL, Chiu CY, John KK, Stahl SE, Rubins KH, McIntyre ABR, Dworkin JP, Lupisella ML, Smith DJ, Botkin DJ, Stephenson TA, Juul S, Turner DJ, Izquierdo F, Federman S, Stryke D, Somasekar S, Alexander N, Yu G, Mason CE, Burton AS. 2017. Nanopore DNA sequencing and genome assembly on the International Space Station. Sci Rep 7:18022. https://doi.org/10.1038/s41598-017-18364-0.
25. Quick J, Quinlan AR, Loman NJ. 2014. A reference bacterial genome dataset generated in the MinION portable single-molecule nanopore sequencer. GigaSci 3:22. https://doi.org/10.1186/2047-217X-3-22.
26. Cornelis S, Gansemans Y, Vander Plaetsen AS, Weymaere J, Willems S, Deforce D, Van Nieuwerburgh F. 2019. Forensic tri-allelic SNP genotyping using nanopore sequencing. Forensic Sci Int Genet 38:204–210. https://doi.org/10.1016/j.fsigen.2018.11.012.
27. Li C, Chng KR, Boey EJ, Ng AH, Wilm A, Nagarajan N. 2016. INC-Seq: accurate single molecule reads using nanopore sequencing. Gigascience 5:34. https://doi.org/10.1186/s13742-016-0140-7.
28. Calus ST, Ijaz UZ, Pinto AJ. 2018. NanoAmpli-Seq: a workflow for amplicon sequencing for mixed microbial communities on the nanopore sequencing platform. Gigascience 7:140. https://doi.org/10.1093/gigascience/giy140.
29. Volden R, Palmer T, Byrne A, Cole C, Schmitz RJ, Green RE, Vollmers C. 2018. Improving nanopore read accuracy with the R2C2 method enables the sequencing of highly multiplexed full-length single-cell cDNA. Proc Natl Acad Sci U S A 115:9726–9731. https://doi.org/10.1073/pnas.1806447115.
30. Pomerantz A, Peñafiel N, Arteaga A, Bustamante L, Pichardo F, Coloma LA, Barrio-Amorós CL, Salazar-Valenzuela D, Prost S. 2018. Real-time DNA barcoding in a rainforest using nanopore sequencing: opportunities for rapid biodiversity assessments and local capacity building. Gigascience 7:giy033. https://doi.org/10.1093/gigascience/giy033.
31. Kilianski A, Haas JL, Corriveau EJ, Liem AT, Willis KL, Kadavy DR, Rosenzweig CN, Minot SS. 2015. Bacterial and viral identification and differentiation by amplicon sequencing on the MinION nanopore sequencer. Gigascience 4:12. https://doi.org/10.1186/s13742-015-0051-z.
32. Ashikawa S, Tarumoto N, Imai K, Sakai J, Kodana M, Kawamura T, Ikebuchi K, Murakami T, Mitsutake K, Maesaki S, Maeda T. 2018. Rapid identification of pathogens from positive blood culture bottles with the MinION nanopore sequencer. J Med Microbiol 67:1589–1595. https://doi.org/10.1099/jmm.0.000855.
33. Benitez-Paez A, Portune KJ, Sanz Y. 2016. Species-level resolution of 16S rRNA gene amplicons sequenced through the MinION portable nanopore sequencer. Gigascience 5:4. https://doi.org/10.1186/s13742-016-0111-z.
34. Benítez-Páez A, Sanz Y. 2017. Multi-locus and long amplicon sequencing approach to study microbial diversity at species level using the MinION portable nanopore sequencer. Gigascience 6:1–12. https://doi.org/10.1093/gigascience/gix043.
35. Kerkhof LJ, Dillon KP, Häggblom MM, McGuinness LR. 2017. Profiling bacterial communities by MinION sequencing of ribosomal operons. Microbiome 5:116. https://doi.org/10.1186/s40168-017-0336-9.
36. Schmidt K, Mwaigwisya S, Crossman LC, Doumith M, Munroe D, Pires C, Khan AM, Woodford N, Saunders NJ, Wain J, O'Grady J, Livermore DM. 2017. Identification of bacterial pathogens and antimicrobial resistance directly from clinical urines by nanopore-based metagenomic sequencing. J Antimicrob Chemother 72:104–114. https://doi.org/10.1093/jac/dkw397.
37. Votintseva AA, Bradley P, Pankhurst L, del Ojo Elias C, Loose M, Nilgiriwala K, Chatterjee A, Smith EG, Sanderson N, Walker TM, Morgan MR. 2017. Same-day diagnostic and surveillance data for tuberculosis via whole genome sequencing of direct respiratory samples. J Clin Microbiol 55:1285–1298. https://doi.org/10.1128/JCM.02483-16.
38. Bronzato Badial A, Sherman D, Stone A, Gopakumar A, Wilson V, Schneider W, King J. 2018. Nanopore sequencing as a surveillance tool for plant pathogens in plant and insect tissues. Plant Dis 102:1648–1652. https://doi.org/10.1094/PDIS-04-17-0488-RE.
39. Hu Y, Green G, Milgate A, Stone E, Rathjen J, Schwessinger B. 2019. Pathogen detection and microbiome analysis of infected wheat using a portable DNA sequencer. Phytobiomes J 3:92–101. https://doi.org/10.1094/PBIOMES-01-19-0004-R.
40. Cusco A, Catozzi C, Vines J, Sanchez A, Francino O. 2018. Microbiota profiling with long amplicons using nanopore sequencing: full-length 16S rRNA gene and whole rrn operon. F1000Res 7:1755. https://doi.org/10.12688/f1000research.16817.1.
41. Deagle BE, Thomas AC, Shaffer AK, Trites AW, Jarman SN. 2013. Quantifying sequence proportions in a DNA-based diet study using Ion Torrent amplicon sequencing: which counts count? Mol Ecol Resour 13:620–633. https://doi.org/10.1111/1755-0998.12103.
42. Schnell IB, Bohmann K, Gilbert M. 2015. Tag jumps illuminated–reducing sequence-to-sample misidentifications in metabarcoding studies. Mol Ecol Resour 15:1289–1303. https://doi.org/10.1111/1755-0998.12402.
43. Costello M, Fleharty M, Abreu J, Farjoun Y, Ferriera S, Holmes L, Granger B, Green L, Howd T, Mason T, Vicente G, Dasilva M, Brodeur W, DeSmet T, Dodge S, Lennon NJ, Gabriel S. 2018. Characterization and remediation of sample index swaps by non-redundant dual indexing on massively parallel sequencing platforms. BMC Genomics 19:332. https://doi.org/10.1186/s12864-018-4703-0.
44. Barnes I, Nest A, Mullett MS, Crous PW, Drenkhan R, Musolin DL, Wingfield MJ. 2016. Neotypification of *Dothistroma septosporum* and epitypi-

fication of *D. pini*, causal agents of *Dothistroma* needle blight of pine. Forest Pathol 46:388–407. https://doi.org/10.1111/efp.12304.
45. Kõljalg U, Nilsson RH, Abarenkov K, Tedersoo L, Taylor AFS, Bahram M, Bates ST, Bruns TD, Bengtsson-Palme J, Callaghan TM, Douglas B, Drenkhan T, Eberhardt U, Dueñas M, Grebenc T, Griffith GW, Hartmann M, Kirk PM, Kohout P, Larsson E, Lindahl BD, Lücking R, Martín MP, Matheny PB, Nguyen NH, Niskanen T, Oja J, Peay KG, Peintner U, Peterson M, Põldmaa K, Saag L, Saar I, Schüßler A, Scott JA, Senés C, Smith ME, Suija A, Taylor DL, Telleria MT, Weiss M, Larsson K-H. 2013. Towards a unified paradigm for sequence-based identification of fungi. Mol Ecol 22:5271–5277. https://doi.org/10.1111/mec.12481.
46. Charalampous T, Richardson H, Kay GL, Baldan R, Jeanes C, Rae D, Grundy S, Turner DJ, Wain J, Leggett RM, Livermore DM. 2018. Rapid diagnosis of lower respiratory infection using nanopore-based clinical metagenomics. BioRxiv https://doi.org/10.1101/387548.
47. Tomlinson JA, Dickinson MJ, Boonham N. 2010. Rapid detection of Phytophthora ramorum and P. kernoviae by two-minute DNA extraction followed by isothermal amplification and amplicon detection by generic lateral flow device. Phytopathology 100:143–149. https://doi.org/10.1094/PHYTO-100-2-0143.
48. Notomi T, Mori Y, Tomita N, Kanda H. 2015. Loop-mediated isothermal amplification (LAMP): principle, features, and future prospects. J Microbiol 53:1–5. https://doi.org/10.1007/s12275-015-4656-9.
49. Reuter JA, Spacek DV, Snyder MP. 2015. High-throughput sequencing technologies. Mol Cell 58:586–597. https://doi.org/10.1016/j.molcel.2015.05.004.
50. Mojarro A, Hachey J, Ruvkun G, Zuber MT, Carr CE. 2018. CarrierSeq: a sequence analysis workflow for low-input nanopore sequencing. BMC Bioinform 19:108. https://doi.org/10.1186/s12859-018-2124-3.
51. Srivathsan A, Hartop E, Puniamoorthy J, Lee WT, Kutty SN, Kurina O, Meier R. 2019. 1D MinION sequencing for large-scale species discovery: 7000 scuttle flies (Diptera: Phoridae) from one site in Kibale National Park (Uganda) revealed to belong to >650 species. bioRxiv https://doi.org/10.1101/622365.
52. Shin J, Lee S, Go MJ, Lee SY, Kim SC, Lee CH, Cho BK. 2016. Analysis of the mouse gut microbiome using full-length 16S rRNA amplicon sequencing. Sci Rep 6:29681. https://doi.org/10.1038/srep29681.
53. Pontefract A, Hachey J, Zuber MT, Ruvkun G, Carr CE. 2018. Sequencing nothing: exploring failure modes of nanopore sensing and implications for life detection. Life Sci Space Res 18:80–86. https://doi.org/10.1016/j.lssr.2018.05.004.
54. White R, Pellefigues C, Ronchese F, Lamiable O, Eccles D. 2017. Investigation of chimeric reads using the MinION. F1000Res 6:631. https://doi.org/10.12688/f1000research.11547.2.
55. Xu X, Stoyanova EI, Lemiesz AE, Xing J, Mash DC, Heintz N. 2018. Species and cell-type properties of classically defined human and rodent neurons and glia. Elife 7:e37551. https://doi.org/10.7554/eLife.37551.
56. Cline LC, Zak DR. 2015. Initial colonization, community assembly and ecosystem function: fungal colonist traits and litter biochemistry mediate decay rate. Mol Ecol 24:5045–5058. https://doi.org/10.1111/mec.13361.
57. Kyaschenko Y, Clemmensen K, Hagenbo A, Karltun E, Lindahl B. 2017. Shift in fungal communities and associated enzyme activities along an age gradient of managed *Pinus sylvestris* stands. ISME J 11:863–874. https://doi.org/10.1038/ismej.2016.184.
58. Jamy M, Foster R, Barbera P, Czech L, Kozlov AM, Stamatakis AM, Bass D, Burki F. 2019. Long metabarcoding of the eukaryotic rDNA operon to phylogenetically and taxonomically resolve environmental diversity. bioRxiv https://doi.org/10.1101/627828.
59. Wurzbacher C, Larsson E, Bengtsson-Palme J, Van den Wyngaert S, Svantesson S, Kristiansson E, Kagami M, Nilsson RH. 2019. Introducing ribosomal tandem repeat barcoding for fungi. Mol Ecol Resour 19:118–127. https://doi.org/10.1111/1755-0998.12944.
60. Karst SM, Dueholm MS, McIlroy SJ, Kirkegaard RH, Nielsen PH, Albertsen M. 2018. Retrieval of a million high-quality, full-length microbial 16S and 18S rRNA gene sequences without primer bias. Nat Biotechnol 36:190–195. https://doi.org/10.1038/nbt.4045.
61. Bradley P, Gordon NC, Walker TM, Dunn L, Heys S, Huang B, Earle S, Pankhurst LJ, Anson L, De Cesare M, Piazza P. 2015. Rapid antibiotic-resistance predictions from genome sequence data for *Staphylococcus aureus* and *Mycobacterium tuberculosis*. Nat Commun 6:10063. https://doi.org/10.1038/ncomms10063.
62. Bahram M, Hildebrand F, Forslund SK, Anderson JL, Soudzilovskaia NA, Bodegom PM, Bengtsson-Palme J, Anslan S, Coelho LP, Harend H, Huerta-Cepas J, Medema MH, Maltz MR, Mundra S, Olsson PA, Pent M, Põlme S, Sunagawa S, Ryberg M, Tedersoo L, Bork P. 2018. Structure and function of the global topsoil microbiome. Nature 560:233–237. https://doi.org/10.1038/s41586-018-0386-6.
63. Simpson JT, Workman RE, Zuzarte PC, David M, Dursi LJ, Timp W. 2017. Detecting DNA cytosine methylation using nanopore sequencing. Nat Methods 14:407. https://doi.org/10.1038/nmeth.4184.
64. Garalde DR, Snell EA, Jachimowicz D, Sipos B, Lloyd JH, Bruce M, Pantic N, Admassu T, James P, Warland A, Jordan M, Ciccone J, Serra S, Keenan J, Martin S, McNeill L, Wallace EJ, Jayasinghe L, Wright C, Blasco J, Young S, Brocklebank D, Juul S, Clarke J, Heron AJ, Turner DJ. 2018. Highly parallel direct RNA sequencing on an array of nanopores. Nat Methods 15:201–208. https://doi.org/10.1038/nmeth.4577.
65. Restrepo-Pérez L, Joo C, Dekker C. 2018. Paving the way to single-molecule protein sequencing. Nat Nanotechnol 13:786. https://doi.org/10.1038/s41565-018-0236-6.
66. Karawdeniya BI, Bandara YN, Nichols JW, Chevalier RB, Dwyer JR. 2018. Surveying silicon nitride nanopores for glycomics and heparin quality assurance. Nat Commun 9:3278. https://doi.org/10.1038/s41467-018-05751-y.
67. Goto Y, Yanagi I, Matsui K, Yokoi T, Takeda KI. 2018. Identification of four single-stranded DNA homopolymers with a solid-state nanopore in alkaline CsCl solution. Nanoscale 10:20844–20850. https://doi.org/10.1039/c8nr04238a.
68. Ioos R, Fabre B, Saurat C, Fourrier C, Frey P, Marçais B. 2010. Development, comparison, and validation of real-time and conventional PCR tools for the detection of the fungal pathogens causing brown spot and red band needle blights of pine. Phytopathology 100:105–114. https://doi.org/10.1094/PHYTO-100-1-0105.
69. White TJ, Bruns TD, Lee S, Taylor J. 1990. Amplification and direct sequencing of fungal ribosomal RNA genes for phylogenetics, p 315–322. *In* Innis MA, Gelfand DH (ed), PCR protocols: a guide to methods and applications. Academic Press, London, United Kingdom.
70. Gardes M, Bruns TD. 1993. ITS primers with enhanced specificity for basidiomycetes–application to the identification of mycorrhizae and rusts. Mol Ecol 2:113–118. https://doi.org/10.1111/j.1365-294X.1993.tb00005.x.
71. Riit T, Tedersoo L, Drenkhan R, Runno-Paurson E, Kokko H, Anslan S. 2016. Oomycete-specific ITS primers for identification and metabarcoding. MycoKeys 14:17–30. https://doi.org/10.3897/mycokeys.14.9244.
72. Riit T, Tedersoo L, Drenkhan R, Runno-Paurson E, Kokko H, Anslan S. 2018. Corrigendum for: "Oomycete-specific ITS primers for identification and metabarcoding" published in MycoKeys. MycoKeys 41:119. https://doi.org/10.3897/mycokeys.41.30558.
73. Tedersoo L, Anslan S. 20 June 2019. Towards PacBio-based pan-eukaryote metabarcoding using full-length ITS sequences. Environ Microbiol Rep https://doi.org/10.1111/1758-2229.12776.
74. Tedersoo L, Lindahl B. 2016. Fungal identification biases in microbiome projects. Environ Microbiol Rep 8:774–779. https://doi.org/10.1111/1758-2229.12438.
75. Vilgalys R, Hester M. 1990. Rapid genetic identification and mapping of enzymatically amplified ribosomal DNA from several Cryptococcus species. J Bacteriol 172:4238–4246. https://doi.org/10.1128/jb.172.8.4238-4246.1990.
76. Anslan S, Bahram M, Hiiesalu I, Tedersoo L. 2017. PipeCraft: flexible open-source toolkit for bioinformatics analysis of custom high-throughput amplicon sequencing data. Mol Ecol Resour 17:e234–e240. https://doi.org/10.1111/1755-0998.12692.
77. Bengtsson-Palme J, Ryberg M, Hartmann M. 2013. Improved software detection and extraction of ITS1 and ITS2 from ribosomal ITS sequences of fungi and other eukaryotes for analysis of environmental sequencing data. Methods Ecol Evol 4:914–919. https://doi.org/10.1111/2041-210X.12073.
78. Edgar RC, Haas BJ, Clemente JC, Quince C, Knight R. 2011. UCHIME improves sensitivity and speed of chimera detection. Bioinformatics 27:2194–2200. https://doi.org/10.1093/bioinformatics/btr381.
79. Edgar RC. 2013. UPARSE: highly accurate OTU sequences from microbial amplicon reads. Nat Methods 10:996–998. https://doi.org/10.1038/nmeth.2604.
80. Camacho C, Coulouris G, Avagyan V, Ma N, Papadopoulos J, Bealer K, Madden TL. 2009. BLAST+: architecture and applications. BMC Bioinformatics 10:421. https://doi.org/10.1186/1471-2105-10-421.